TGAL-TR-83-7

THE LOW FREQUENCY SPECTRAL MINIMUM IN UNDERGROUND EXPLOSION P SPECTRA

Gene Smart

TELEDYNE GEOTECH
Alexandria Laboratories
314 Montgomery Street
Alexandria, VA 22314

12 January 1984

Technical Report

APPROVED FOR PUBLIC RELEASE; DISTRIBUTION UNLIMITED.

Prepared for:
DEFENSE ADVANCED RESEARCH PROJECTS AGENCY
1400 Wilson Boulevard
Arlington, VA 22209

Monitored by:
AFTAC/TG
Patrick Air Force Base
Florida 32925

Sponsored by
Defense Advanced Research Project Agency (DARPA)
ARPA Order No. 4398

UNCLASSIFIED
SECURITY CLASSIFICATION OF THIS PAGE

REPORT DOCUMENTATION PAGE

1a. REPORT SECURITY CLASSIFICATION UNCLASSIFIED	1b. RESTRICTIVE MARKINGS
2a. SECURITY CLASSIFICATION AUTHORITY 2b. DECLASSIFICATION/DOWNGRADING SCHEDULE	3. DISTRIBUTION/AVAILABILITY OF REPORT Approved for public release; distribution is unlimited.
4. PERFORMING ORGANIZATION REPORT NUMBER(S) TGAL-TR-83-7	5. MONITORING ORGANIZATION REPORT NUMBER(S)
6a. NAME OF PERFORMING ORGANIZATION TELEDYNE GEOTECH Alexandria Laboratories 6b. OFFICE SYMBOL (If applicable)	7a. NAME OF MONITORING ORGANIZATION AFTAC/TG
6c. ADDRESS (City, State and ZIP Code) 214 Montgomery Street Alexandria, Virginia 22314	7b. ADDRESS (City, State and ZIP Code) Patrick Air Force Base Florida 32925
8a. NAME OF FUNDING/SPONSORING ORGANIZATION DARPA 8b. OFFICE SYMBOL (If applicable)	9. PROCUREMENT INSTRUMENT IDENTIFICATION NUMBER F08606-83C-0004
8c. ADDRESS (City, State and ZIP Code) 1400 Wilson Boulevard Arlington, Virginia 22209	10. SOURCE OF FUNDING NOS. PROGRAM ELEMENT NO.: — PROJECT NO.: VT/3709/B/PMP TASK NO.: — WORK UNIT NO.: —
11. TITLE (Include Security Classification) (See Block 16)	
12. PERSONAL AUTHOR(S) Gene Smart	
13a. TYPE OF REPORT Technical 13b. TIME COVERED FROM Nov. 82 TO Nov. 83	14. DATE OF REPORT (Yr., Mo., Day) 84-01-12 15. PAGE COUNT 50
16. SUPPLEMENTARY NOTATION THE LOW FREQUENCY SPECTRAL MINIMUM IN UNDERGROUND EXPLOSION P SPECTRA	

17. COSATI CODES			18. SUBJECT TERMS (Continue on reverse if necessary and identify by block number)
FIELD	GROUP	SUB. GR.	
08	11		Zero-Frequency Spectral Hole; pP Interference, Depth of Burial; and Amchitka test

19. ABSTRACT (Continue on reverse if necessary and identify by block number)

We confirm that a very low frequency discriminant, i.e., the hole due to pP interference, located at the lower extreme of underground nuclear explosion spectra, is preserved in short-period seismic recordings. This is shown repeatedly, from subarray to subarray, in comparisons of LONGSHOT with a control earthquake, in recordings of those events made at LASA. The discriminant, previously neglected as falling outside seismometer spectral range, is available with present recording systems. To isolate the pP effect for observation the explosion spectra are, in effect, divided by the spectra of the control earthquake, removing the interference of earth and instrument responses. It is not clear whether use of a control earthquake is unavoidable. Keywords include:

20. DISTRIBUTION/AVAILABILITY OF ABSTRACT UNCLASSIFIED/UNLIMITED ☒ SAME AS RPT. ☐ DTIC USERS ☐	21. ABSTRACT SECURITY CLASSIFICATION UNCLASSIFIED
22a. NAME OF RESPONSIBLE INDIVIDUAL Capt. Kenneth M. Ols	22b. TELEPHONE NUMBER (Include Area Code) (305) 494-5263 22c. OFFICE SYMBOL TGR

DD FORM 1473, 83 APR — EDITION OF 1 JAN 73 IS OBSOLETE.

UNCLASSIFIED
SECURITY CLASSIFICATION OF THIS PAGE

TABLE OF CONTENTS

	Page
LIST OF FIGURES	iv
INTRODUCTION	1
OBSERVATIONS OF THE pP VERY LOW FREQUENCY HOLE IN SHORT-PERIOD EXPLOSION SPECTRA	5
AN ANOMALOUS PEAK AT ZERO FREQUENCY IN LASA SHORT-PERIOD SPECTRA	18
CORRECTING FOR BEAMSUM SPECTRAL BIAS	25
CONCLUSIONS AND RECOMMENDATIONS	29
REFERENCES	30
APPENDIX: THE CORRECTION FOR BEAMSUM SPECTRAL BIAS	31
DISTRIBUTION LIST	

LIST OF FIGURES

Figure No.	Title	Page
1	The effect on a flat signal spectrum of a reflection delayed 0.55 sec after the signal itself, with reflectivity equal to 1.0. (0.55 sec is the observed pP delay for LONGSHOT; Cohen, 1970). The actual LONGSHOT spectrum, shown in Figures 2-9, rolls off toward zero frequency at about the same rate, with respect to the control earthquake.	6
2	From LASA subarray A0 beamsums: the P spectrum of LONGSHOT superposed on that of the nearby control earthquake of December 12, 1965. The LONGSHOT spectrum has been shifted down to make its peak coincide with that of the earthquake, to which the vertical scale applies. Note that LONGSHOT rolls-off toward zero frequency at about the same rate, with respect to the earthquake, as does the anticipated zero-frequency pP hole, shown in Figure 1, with respect to a flat spectrum. There is no correction made for instrument response; 5-point smoothing is applied.	8
3	From LASA subarray B3 beamsums: the P spectrum of LONGSHOT superposed on that of the nearby control earthquake of December 12, 1965. Note the roll-off of LONGSHOT toward zero frequency, with respect to the quake, due to pP interference. Refer to Figure 2.	9
4	From LASA subarray D3 beamsums: the P spectrum of LONGSHOT superposed on that of the nearby control earthquake of December 12, 1965. Note the roll-off of LONGSHOT toward zero frequency, with respect to the quake, due to pP interference. Refer to Figure 2.	10
5	From LASA subarray E2 beamsums: the P spectrum of LONGSHOT superposed on that of the nearby control earthquake of December 12, 1965. Note the roll-off of LONGSHOT toward zero frequency, with respect to the quake, due to pP interference. Refer to Figure 2.	11

LIST OF FIGURES (continued)

Figure No.	Title	Page
6	From LASA subarray E3 beamsums: the P spectrum of LONGSHOT superposed on that of the nearby control earthquake of December 12, 1965. Note the roll-off of LONGSHOT toward zero frequency, with respect to the quake, due to pP interference. Refer to Figure 2.	12
7	From LASA subarray E4 beamsums: the P spectrum of LONGSHOT superposed on that of the nearby control earthquake of December 12, 1965. Note the roll-off of LONGSHOT toward zero frequency, with respect to the quake, due to pP interference. Refer to Figure 2.	13
8	From LASA subarray F1 beamsums: the P spectrum of LONGSHOT superposed on that of the nearby control earthquake of December 12, 1965. Note the roll-off of LONGSHOT toward zero frequency, with respect to the quake, due to pP interference. Refer to Figure 2.	14
9	From LASA subarray F3 beamsums: the P spectrum of LONGSHOT superposed on that of the nearby control earthquake of December 12, 1965. Note the roll-off of LONGSHOT toward zero frequency, with respect to the quake, due to pP interference. Refer to Figure 2.	15
10	The LASA A0-subarray beamsum spectra for the LONGSHOT P wave and the preceding noise. The plus symbols represent the P-wave spectrum.	17
11	The LASA D4-subarray beamsum spectrum of LONGSHOT corrected for instrument response. Observe the large peak at zero frequency. Similar anomalous peaks appear in the spectra of the control earthquake, the shot beamsum residuals, and the pre-shot noise, scaled in each case to the rest of the spectrum, as shown in Figures 12, 13, and 14. The window length is 51.2 sec. There is no smoothing.	19
12	The LASA C1-subarray beamsum spectrum of the control earthquake corrected for instrument response. Observe the peak at zero frequency. Similar anomalous peaks appear in the spectra of LONGSHOT, the shot beamsum residuals, and the pre-shot noise, scaled in each case to the rest of the spectrum, as shown in Figures 11, 13, and 14. The window length is 51.2 sec. There is no smoothing.	20

LIST OF FIGURES (continued)

Figure No.	Title	Page
13	The mean spectrum of the beamsum residuals of LONGSHOT as recorded at the LASA D4-subarray, corrected for instrument response. Observe the large peak at zero frequency. Similar anomalous peaks appear in the spectra of LONGSHOT itself, the control earthquake, and the pre-shot noise, scaled in each case to the rest of the spectrum, as shown in Figures 11, 12, and 14. The window length is 51.2 sec. There is no smoothing.	21
14	The LASA A0-subarray beamsum spectrum of pre-LONGSHOT noise corrected for instrument response. Observe the peak at zero frequency. Similar anomalous peaks appear in the spectra of LONGSHOT itself, the control earthquake, and the shot beamsum residuals, scaled in each case to the rest of the spectrum, as shown in Figures 11, 12, and 13. The window length is 51.2 sec. There is no smoothing.	22
15	To the left, above, is the LASA A0-subarray beamsum spectrum of the LONGSHOT P-wave corrected for instrument response. Observe the pP hole around 1.9 Hz, and the anomalous peak at zero frequency. The window length is 6.4 sec. There is no smoothing. At the right, above, is the F spectrum for the same window. Observe the pP hole around 1.9 Hz and also that at zero frequency. The latter hole indicates the likelihood that, as zero frequency is approached, less and less of the estimated energy in that part of the spectrum is indeed part of the signal, even though the 25 waveforms in the sum are beamed right at LONGSHOT. This suggests that the F statistic may be used to estimate just how much of the spectral energy at a given frequency is spurious, and to correct for it. That idea is developed in the Appendix.	23
16	To the left, above, is the LASA B4-subarray beamsum spectrum for LONGSHOT, corrected for instrument response. Observe the sharp peak at zero frequency. The window length is 51.2 sec. There is no smoothing. At the right, above, is the same spectrum corrected for the beamsum bias by means of the F statistic (as a function of frequency). Observe that the sharp peak at zero frequency is now absent, replaced by a hole.	26

LIST OF FIGURES (continued)

Figure No.	Title	Page
17	To the left, above, is the LASA F4-subarray beamsum spectrum for LONGSHOT, corrected for instrument response. Observe the large peak at zero frequency. The window length is 51.2 sec. There is no smoothing. At the right, above, is the same spectrum corrected for the beamsum bias by means of the F statistic (as a function of frequency). Observe that the large peak at zero frequency is now absent, replaced by a hole.	27

(THIS PAGE INTENTIONALLY LEFT BLANK)

INTRODUCTION

The first signal, i.e., the P wave, arriving at a seismograph from a shallow, teleseismic event will be mixed with its own reflection off the surface of the earth. The recorded signal, $s(t)$, may be represented as the P wave, $p(t)$, of the event plus its undistorted echo reversed in phase and delayed by time d:

$$s(t) = p(t) - r * p(t-d) \tag{1}$$

where r is the reflection coefficient, which can range from 0 to 1. If $P(\omega)$ is the power spectrum of p, then the spectrum of the signal s is (Cohen, 1970):

$$P(\omega) * [\, 1 + r^2 - 2*r*cos\ (\omega * d)]$$

If the reflectivity, r, is 1, as it tends to be at the lower frequencies, then the spectrum of the recorded signal is the spectrum of the P wave shaped by the factor

$$2[\, 1 - cos\ (\omega * d)]$$

Thus the signal spectrum will go to zero at every frequency, ω, at which

$$\omega = 2 * \pi * n / d \quad (n = \pm 0,1,2,3,...) \tag{2}$$

If the power spectrum of the P wave itself is flat, then the spectrum of the recorded signal will have a sinusoidal shape. There will be a series of regularly spaced holes centered on frequencies the locations of which will depend on d, the delay. That is, the hole locations will depend on d except for the hole centered on frequency zero, which is, of course, always at the one location.

The factor shaping the signal *amplitude* spectrum, i.e., the square root of the power spectrum, is

$$\sqrt{2} * [\, 1 - cos(\omega * d)]^{0.5}$$

The size of this hole produced in the amplitude spectrum by the interference of the reflected signal may be characterized by its half width, i.e., its width where it has reduced the spectrum by one half. This occurs when

$$\omega = (2 * \pi * n \pm \pi / 3) / d \tag{3}$$

As an example, the size of the holes produced in an amplitude spectrum by an echo delayed 0.55 seconds is 0.6 hertz. That is, they will have a half-width of 0.6 hertz. In general, the shallower the event the wider the spectral hole.

The low-frequency hole in the P-wave spectrum of shallow seismic events is a potentially powerful discriminant for distinguishing the seismic signals of earthquakes from those of underground nuclear explosions. When the hole is diagnostic of a depth below the reach of present technology the event must a natural earthquake. Some of the advantages of the low-frequency hole as a discriminant are:

a) At low frequencies the coefficient of reflectivity approaches 1.0, ensuring that the spectral hole is not obscured by low reflectivity at the earth's surface, as it may be for the fundamental mode and its harmonics, at some test sites.

b) Unlike the fundamental mode of pP interference and its harmonics, the component at the lower extreme has an unequivocal location in the spectrum. There can be confusion about the position, and therefore about the identity, of the other holes produced by interference. The hole of the fundamental mode in the LONGSHOT spectrum, for instance, was anomalously located (Cohen, 1970). But the very low frequency component, because of its unique position cannot be confused with spurious holes in the spectrum, such as those produced by discrete multipaths. (An example of such multipathing is found in the record of LONGSHOT at Eskdalemuir, Scotland, which reveals two discrete direct ray-paths between the source and the receiver; Douglas et al., 1972.) Though multipathing can cause spectral scalloping, it does not produce a hole at the lower extreme of the spectrum.

c) Scattering of surface-waves to body-waves in the vicinity of the event is reduced at the lower frequencies since the scatterers in the crust are smaller than the corresponding wave-lengths. This ensures that energy which has not undergone the pP cancellation does not fill in the spectral hole and conceal it, as it may do at the fundamental frequency and its harmonics.

d) It cannot be disguised. The flat spectrum characteristic of deeper events cannot be simulated as can a discriminant such as complexity, which characterizes earthquakes but which, conceptually at least, can be imitated by an array of nuclear shots fired in rapid sequence.

The difficulties associated with the use of the very low frequency hole as a discriminant are these:

1) The low frequency part of the signal is not optimumly recorded. The short-period recording systems in the field have responses which drop off sharply at the low end of t [illegible]um. The long-period systems operate just in the frequency range of interest but at low gai[illegible] that permit the observation of the P waves of only larger events.

2) The six-second microseisms dominate precisely the portion of the spectrum of interest.

3) Though there are now mid-period recording systems going into the field, they are not installed in arrays and thus their data are not susceptible of the analytic techniques required to overcome the microseism noise, which is well organized.

The problems associated with the very low frequency discriminant are not, however, necessarily insuperable. Since the six-second microseisms are well organized they are susceptible to array processing, and may thus be removable. There are abundant data, both past and present, from short-period arrays. These records will admit of array processing which may allow both the suppression of the microseisms and the reconstitution of the low-frequency end of the signal spectrum.

OBSERVATIONS OF THE pP VERY LOW FREQUENCY HOLE IN SHORT-PERIOD EXPLOSION SPECTRA

In the present research to evaluate the feasibility of using the very low frequency hole as a discriminant we first examine the spectra of events large enough to overwhelm the microseism noise. We do this simply to verify that there is such a hole to be observed in the short-period data, given the steep roll-off at the low-frequency end of the response of the short-period systems. We choose the LASA short-period subarray records of the Amchitka test LONGSHOT. The event is suitable because 1) it is at teleseismic distance, 2) it is large enough to be just within the dynamic range of the system, thus affording the maximum signal-to-noise ratio, and, 3) at the time of LONGSHOT the entire array was still in place, having 25 short-period vertical seismometers per subarray. Also, a control event is available for comparison. An earthquake took place a few months afterward, on December 12, 1965, within about a degree of LONGSHOT and 0.65 magnitude unit smaller, and the LASA recording of it has survived. The estimated depth of the earthquake is 49 kilometers.

An idea of the appearance of the spectral hole we may expect to see is given in Figure 1, which shows the anticipated effect, on an otherwise flat amplitude spectrum, of pP interference for the depth of burial of LONGSHOT. The expression for this spectrum was derived in the introduction. A coefficient of reflectivity of 1.0 is assumed; the event is at teleseismic distance. The amplitude spectrum of *LONGSHOT* should have a hole of this size, shape and location superposed on it.

However, the signal as recorded has been reshaped by earth response and instrument response, which will distort the features we are attempting to identify. Nevertheless, the control earthquake has also been through the same physical filters and its spectrum can be used as a template against which to compare the shot spectrum to locate and identify its distinctive features. Since the anticipated source spectrum of an earthquake is flat at the lower end, up to the corner frequency, we can expect LONGSHOT to have an amplitude spectrum which differs in shape from the spectrum of

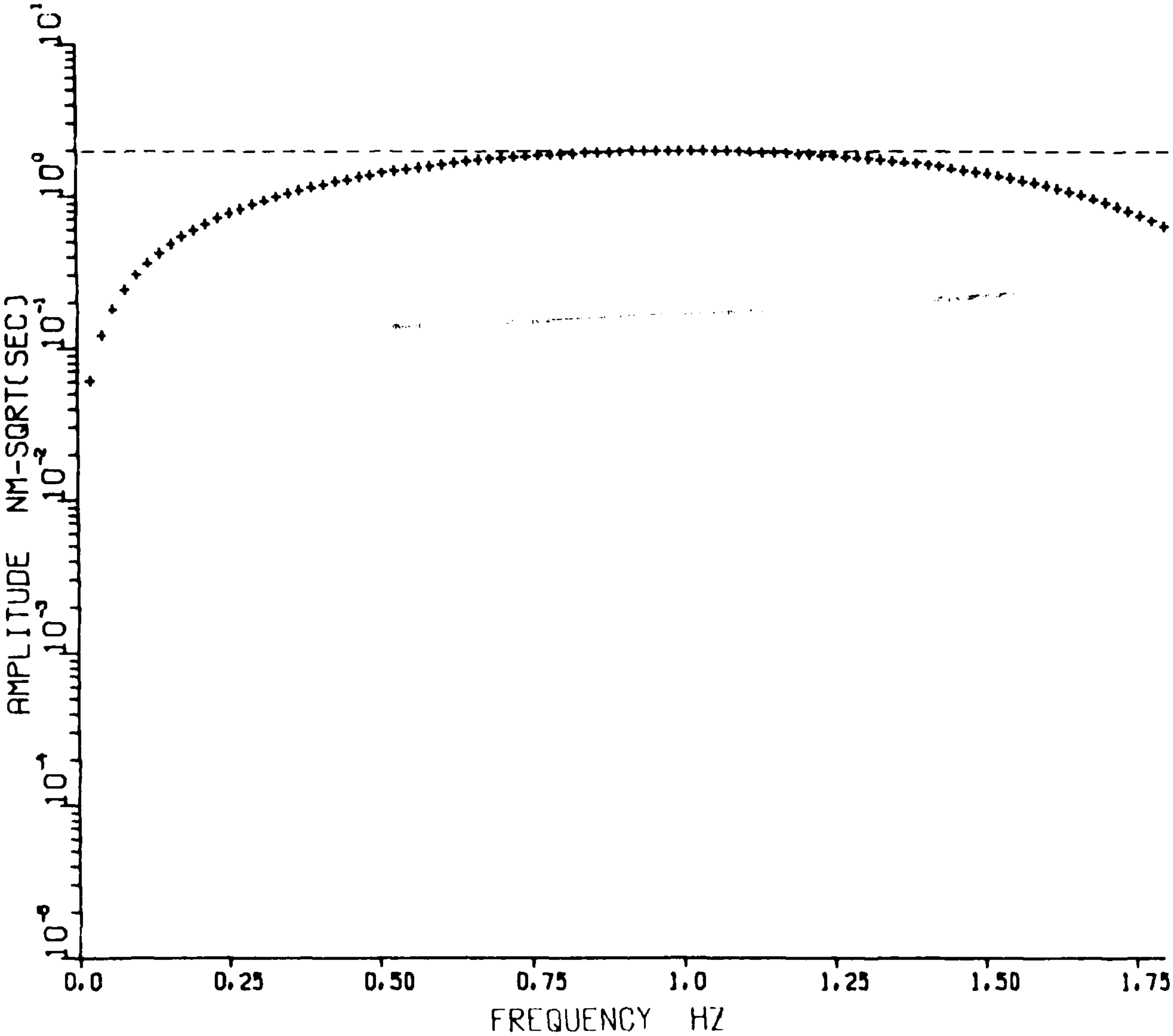

NO INST CORRECTION 0 PT SMOOTHING

Figure 1. The effect on a flat signal spectrum of a reflection delayed 0.55 sec after the signal itself, with reflectivity equal to 1.0. (0.55 sec is the observed pP delay for LONGSHOT; Cohen, 1970). The actual LONGSHOT spectrum, shown in Figures 2-9, rolls off toward zero frequency at about the same rate, with respect to the control earthquake.

the control earthquake as Figure 1 differs from constant amplitude.

For that comparison Figures 2 through 9 juxtapose actual P-wave spectra of LONGSHOT with those of the control earthquake. Each figure contains the P-wave beamsum spectrum of the shot superposed on that of the earthquake, both from records at a specified LASA subarray. The two events were of different magnitude and so to facilitate the comparison of the spectral shapes the LONGSHOT spectra in these figures have been adjusted vertically such that the maximum amplitude of the shot coincides with that of the earthquake. Thus the scale on the ordinate applies only to the earthquake. (The adjustment is entirely graphical to facilitate visual comparison; the shot data themselves were not normalized to the earthquakes'.)

We use subarray beamsums rather than single traces for computing these spectra. In so doing, we maximize the signal-to-noise ratios, but we also avail ourselves of statistical control over the signal estimates by means of F spectra, which are defined for beamsum spectra but not for those of single traces, as discussed below. The usual limitation on beamforming that a trace can only be shifted an integral number of the data sample-intervals is avoided here. To form the beam we shift a given trace the integral number of sample intervals nearest to the exact time-delay required, and then we Fourier transform that record and shift the remaining fraction of a sample interval in the frequency domain. Thus we avoid possible artifacts in the spectra that might result from beaming inaccuracies, especially at higher frequencies.

In each of these figures the spectrum of the LONGSHOT P wave can be seen to fall below the earthquake spectrum uniformly and steadily, from the peak at about 1.0 Hz back toward zero frequency. Between that peak and 0.15 Hz the shot spectrum drops off about -14db, on the average, with respect to the earthquake. Note that this is equal to the anticipated fall in amplitude, shown in Figure 1, where from the peak amplitude at 1.0 Hz the spectrum drops to about -13db at 0.15 Hz. This is the observation we sought to make. The very low frequency discriminant survived the filtering effects of

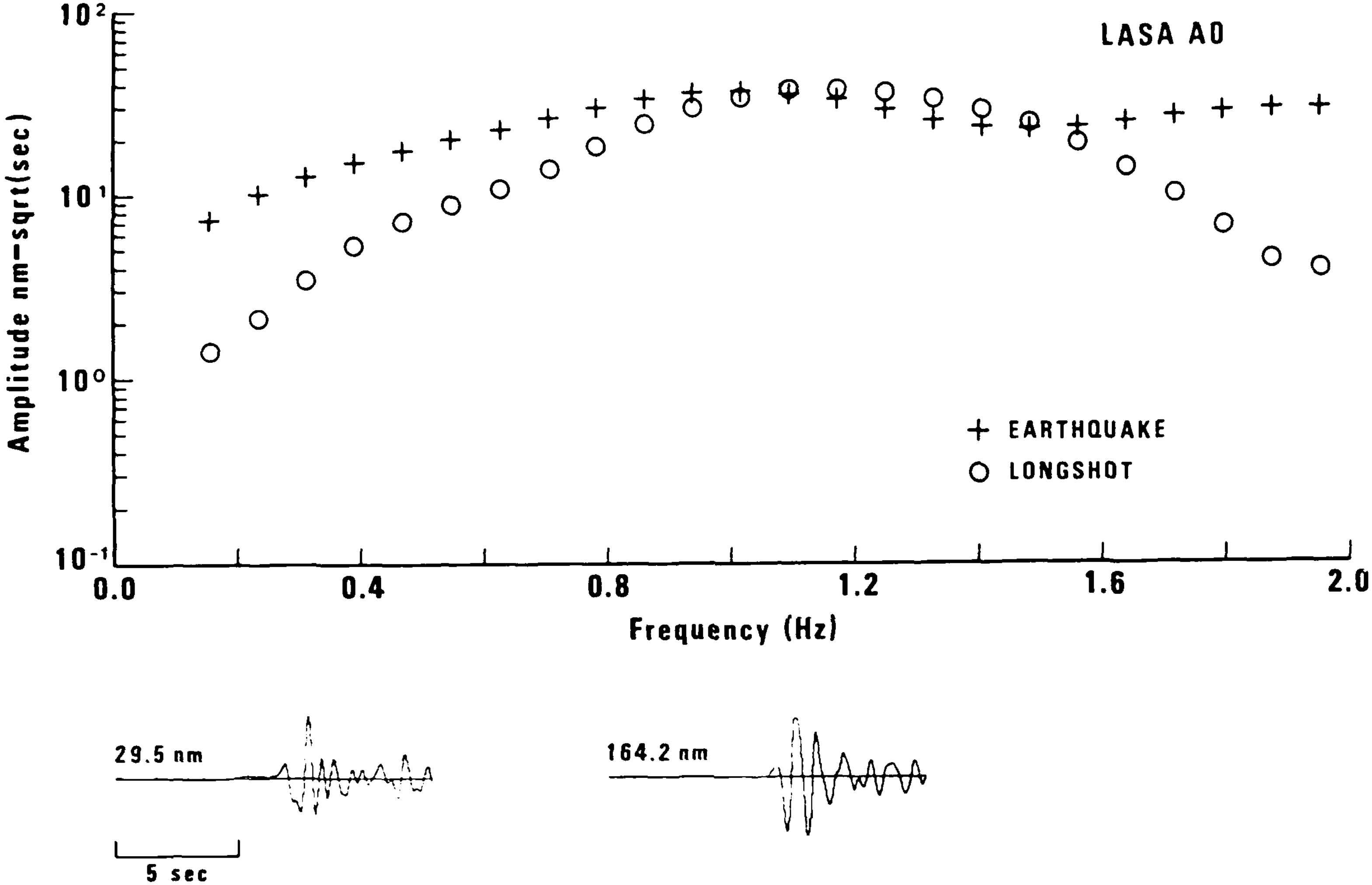

Figure 2. From LASA subarray A0 beamsums: the P spectrum of LONGSHOT superposed on that of the nearby control earthquake of December 12, 1965. The LONGSHOT spectrum has been shifted down to make its peak coincide with that of the earthquake, to which the vertical scale applies. Note that LONGSHOT rolls-off toward zero frequency at about the same rate, with respect to the earthquake, as does the anticipated zero-frequency pP hole, shown in Figure 1, with respect to a flat spectrum. There is no correction made for instrument response; 5-point smoothing is applied.

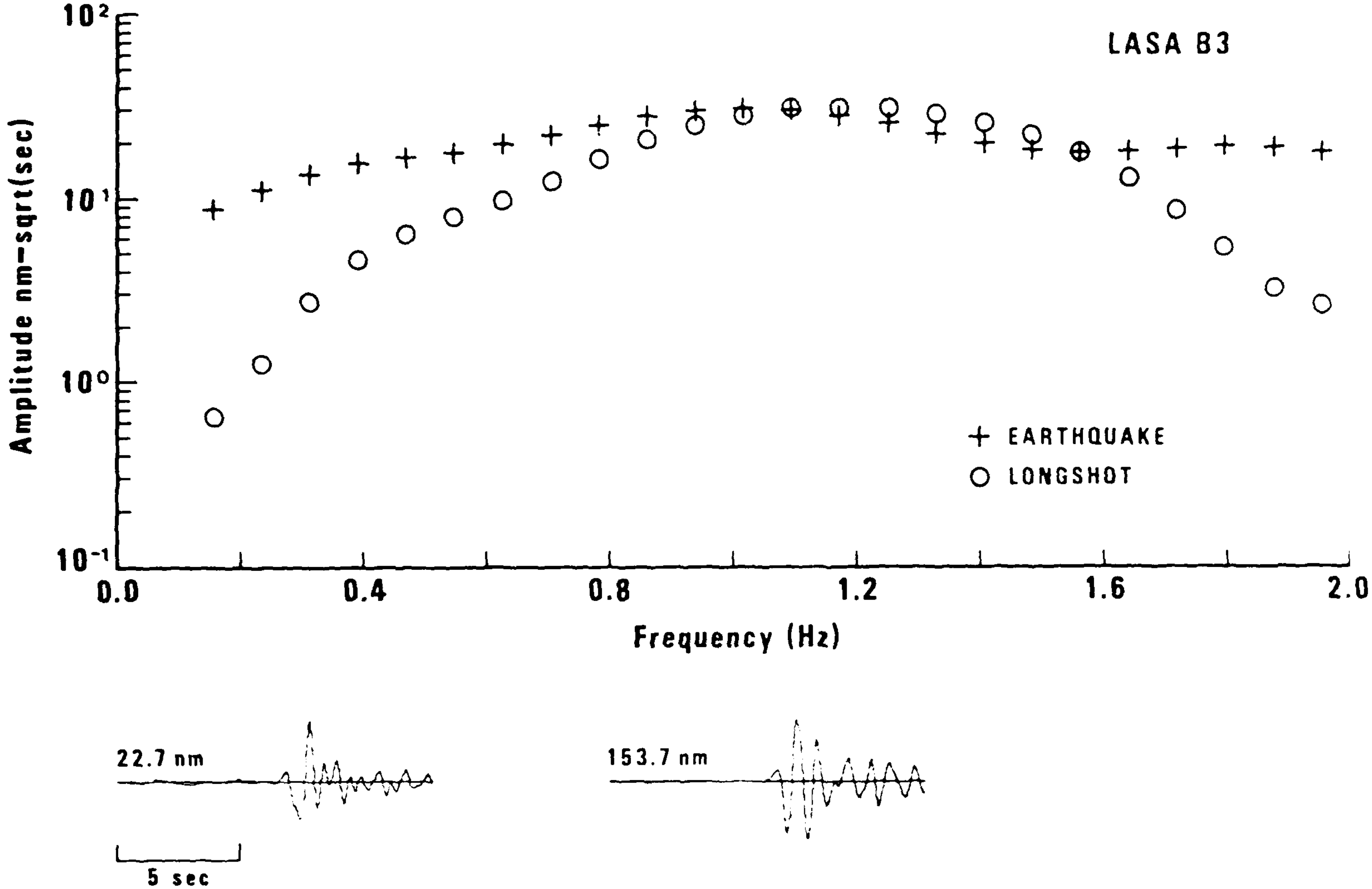

Figure 3. From LASA subarray B3 beamsums: the P spectrum of LONGSHOT superposed on that of the nearby control earthquake of December 12, 1965. Note the roll-off of LONGSHOT toward zero frequency, with respect to the quake, due to pP interference. Refer to Figure 2.

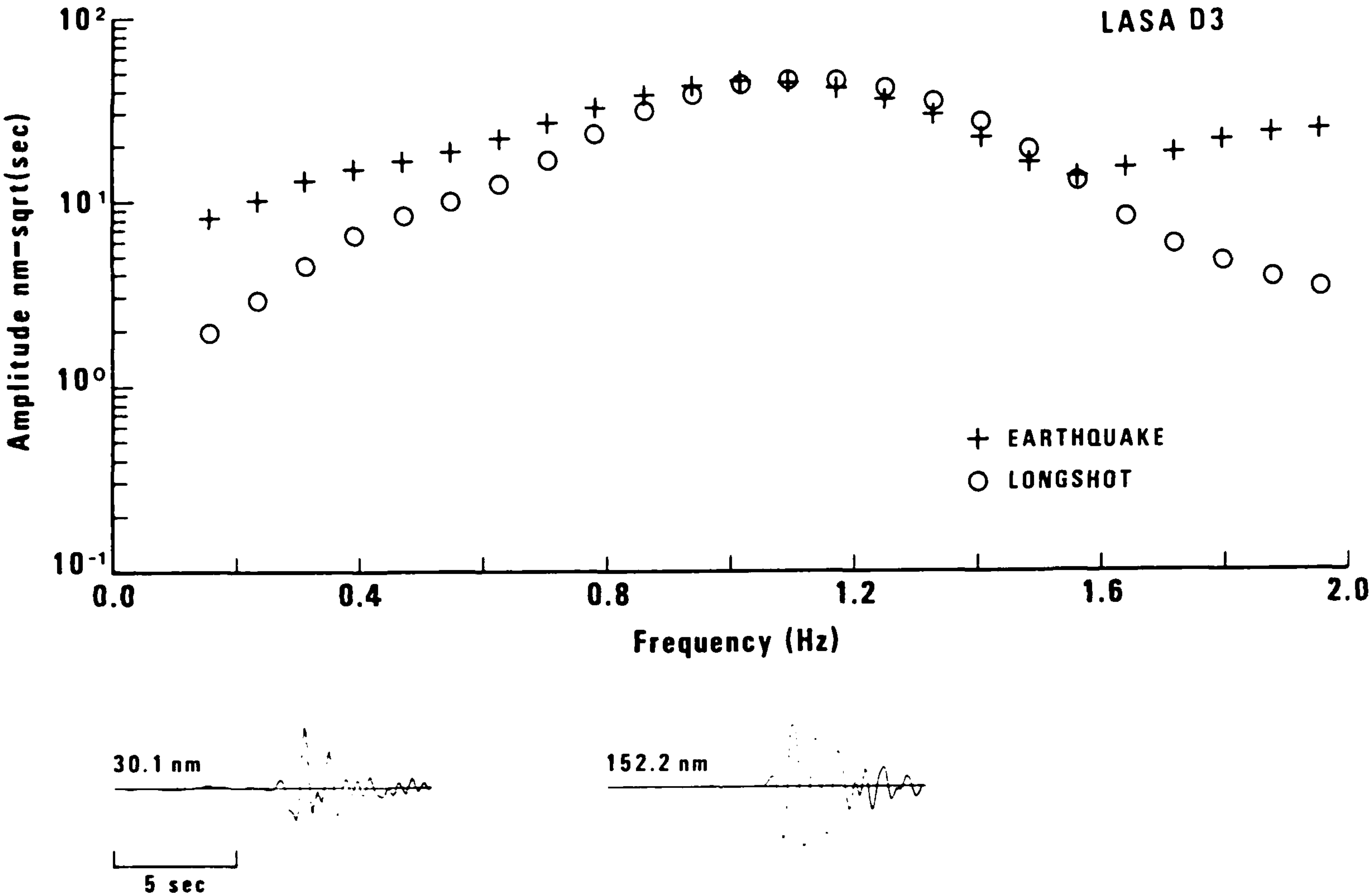

Figure 4. From LASA subarray D3 beamsums: the P spectrum of LONGSHOT superposed on that of the nearby control earthquake of December 12, 1965. Note the roll-off of LONGSHOT toward zero frequency, with respect to the quake, due to pP interference. Refer to Figure 2.

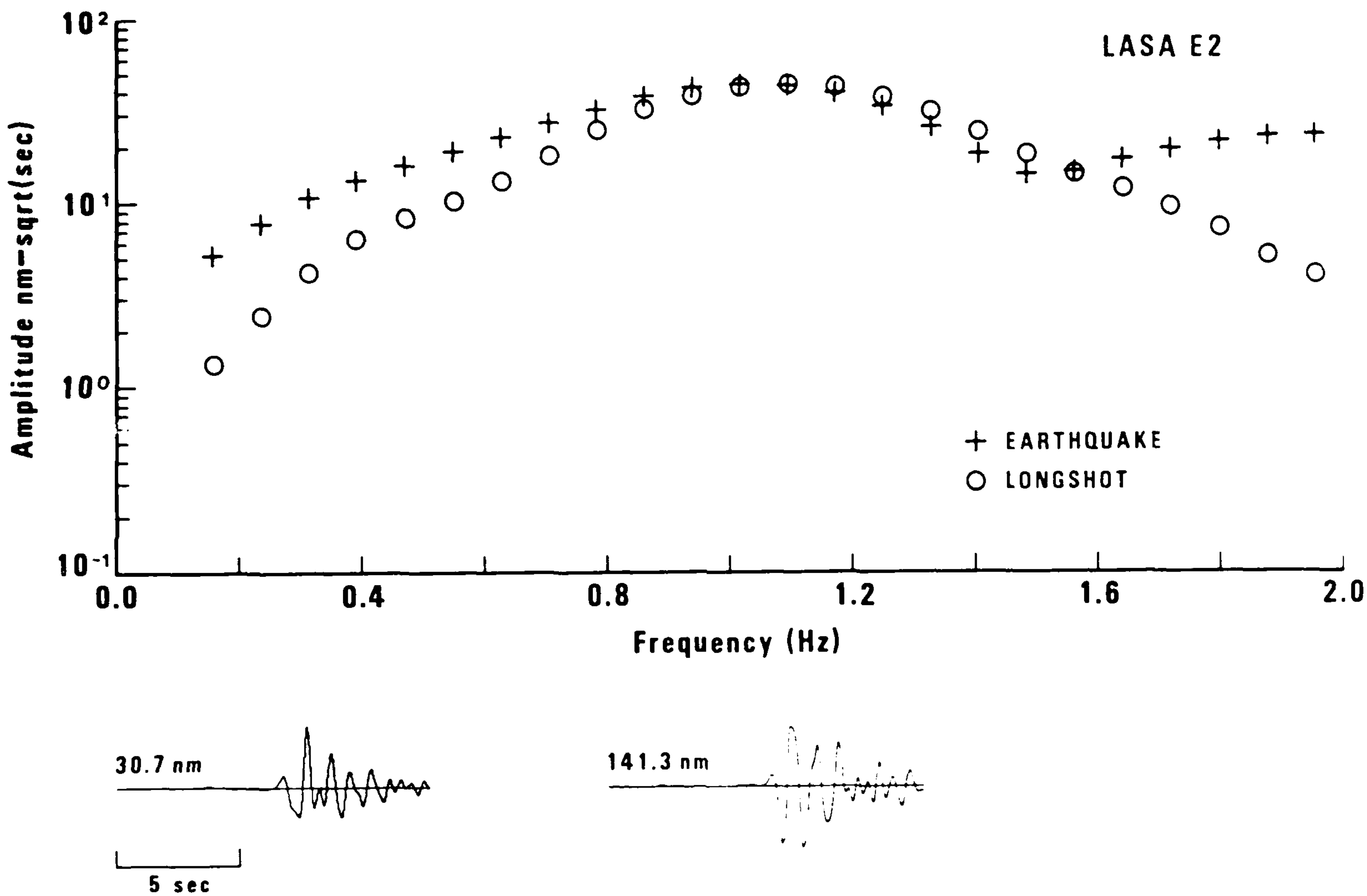

Figure 5. From LASA subarray E2 beamsums: the P spectrum of LONGSHOT superposed on that of the nearby control earthquake of December 12, 1965. Note the roll-off of LONGSHOT toward zero frequency, with respect to the quake, due to pP interference. Refer to Figure 2.

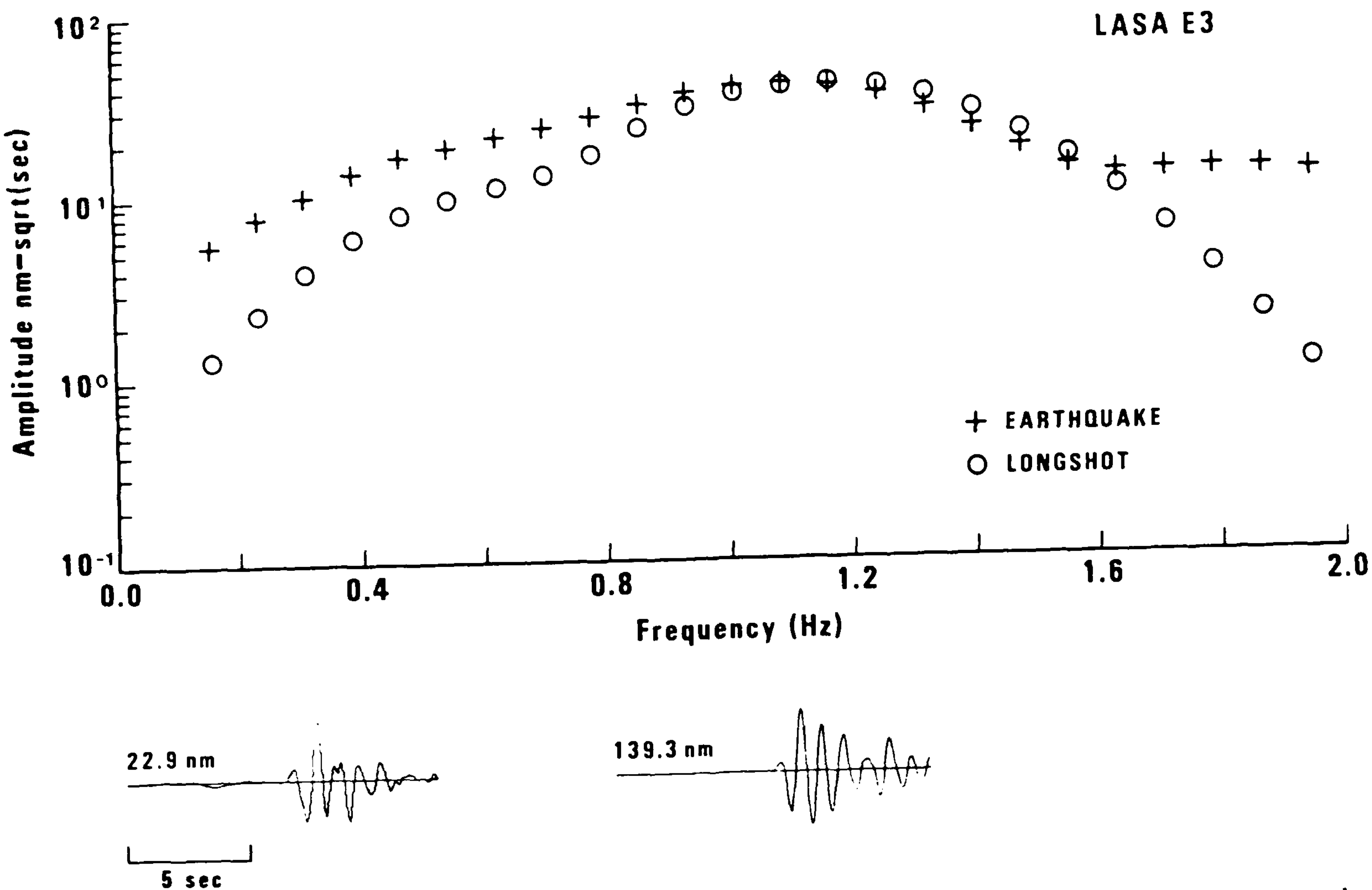

Figure 6. From LASA subarray E3 beamsums: the P spectrum of LONGSHOT superposed on that of the nearby control earthquake of December 12, 1965. Note the roll-off of LONGSHOT toward zero frequency, with respect to the quake, due to pP interference. Refer to Figure 2.

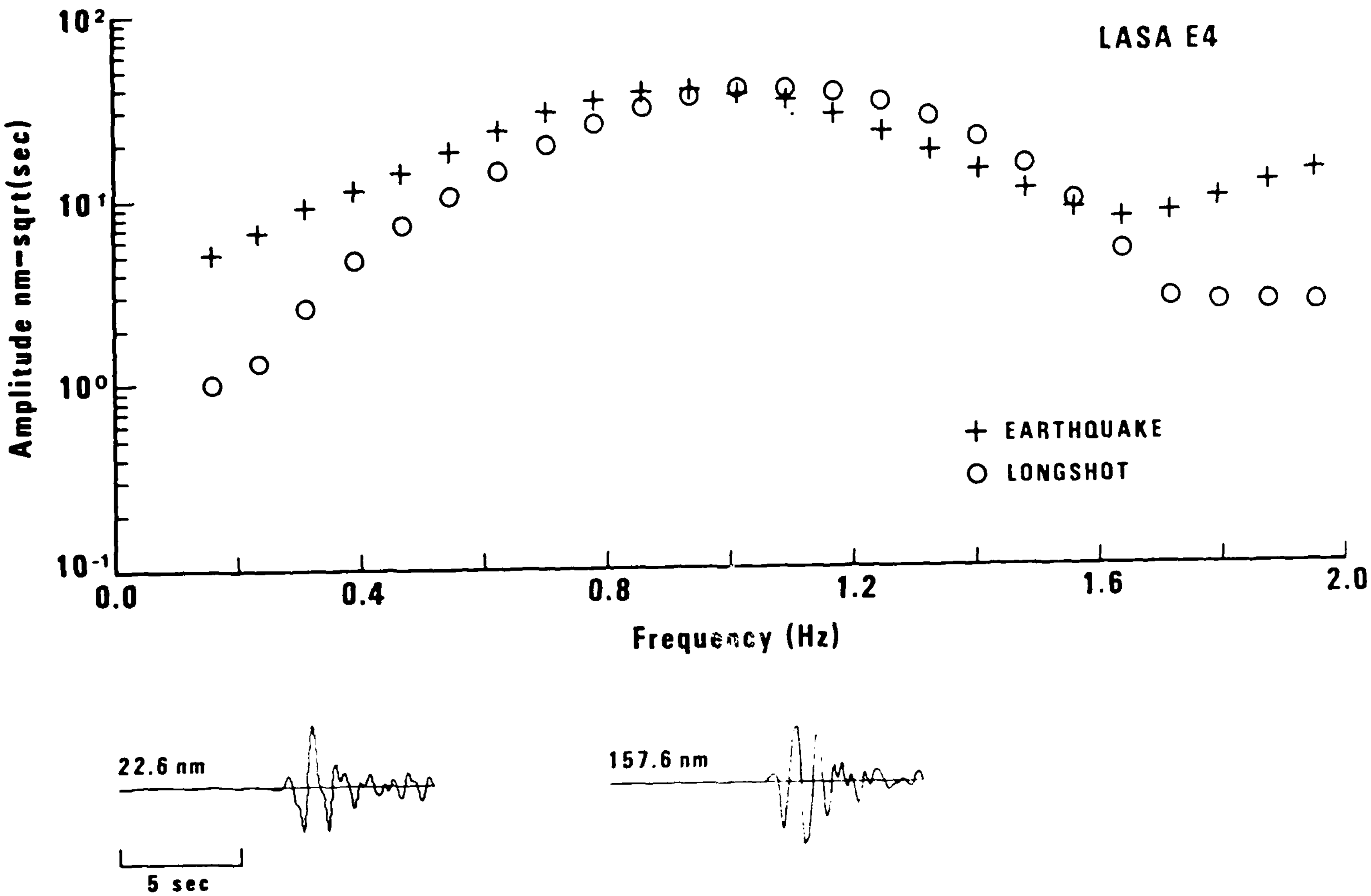

Figure 7. From LASA subarray E4 beamsums: the P spectrum of LONGSHOT superposed on that of the nearby control earthquake of December 12, 1965. Note the roll-off of LONGSHOT toward zero frequency, with respect to the quake, due to pP interference. Refer to Figure 2.

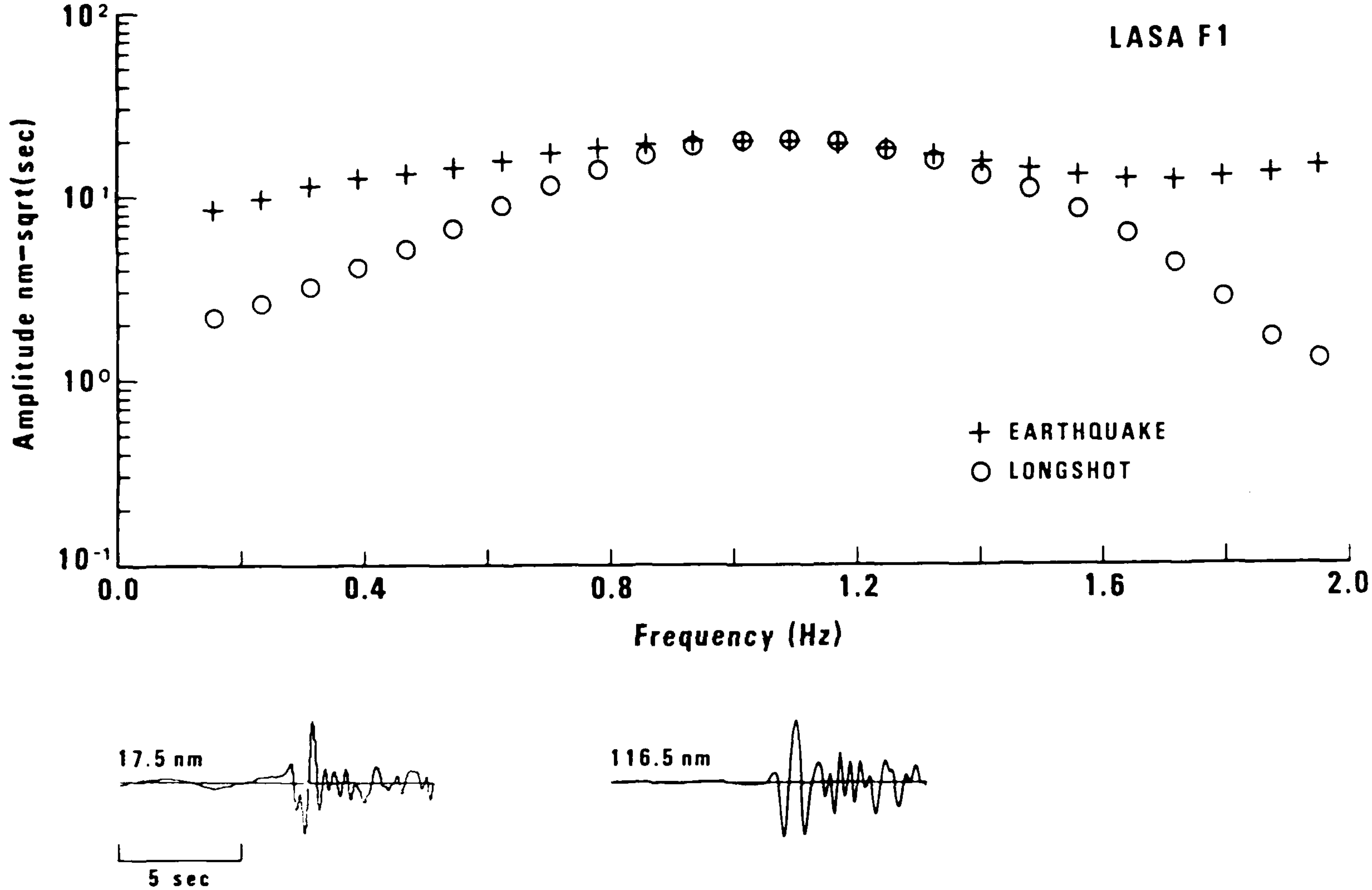

Figure 8. From LASA subarray F1 beamsums: the P spectrum of LONGSHOT superposed on that of the nearby control earthquake of December 12, 1965. Note the roll-off of LONGSHOT toward zero frequency, with respect to the quake, due to pP interference. Refer to Figure 2.

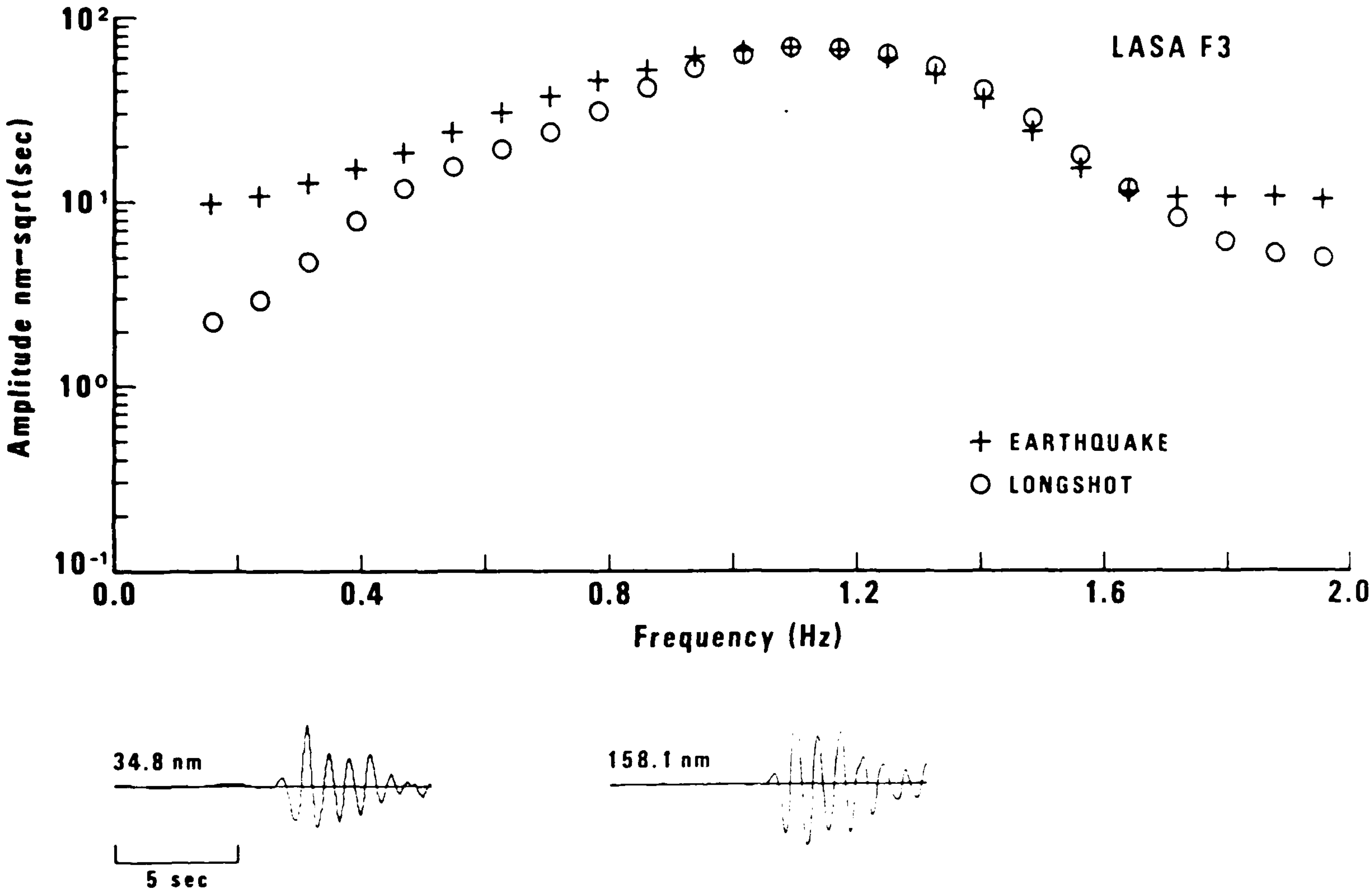

Figure 9. From LASA subarray F3 beamsums: the P spectrum of LONGSHOT superposed on that of the nearby control earthquake of December 12, 1965. Note the roll-off of LONGSHOT toward zero frequency, with respect to the quake, due to pP interference. Refer to Figure 2.

transmission through the earth and through the sensor, in spite of being only marginally within the range of the seismometer frequency response. Note that in each of these records in Figures 2 through 9, both for the shot and for the earthquake, the noise is at least -20db below the signal, as shown in the example in Figure 10.

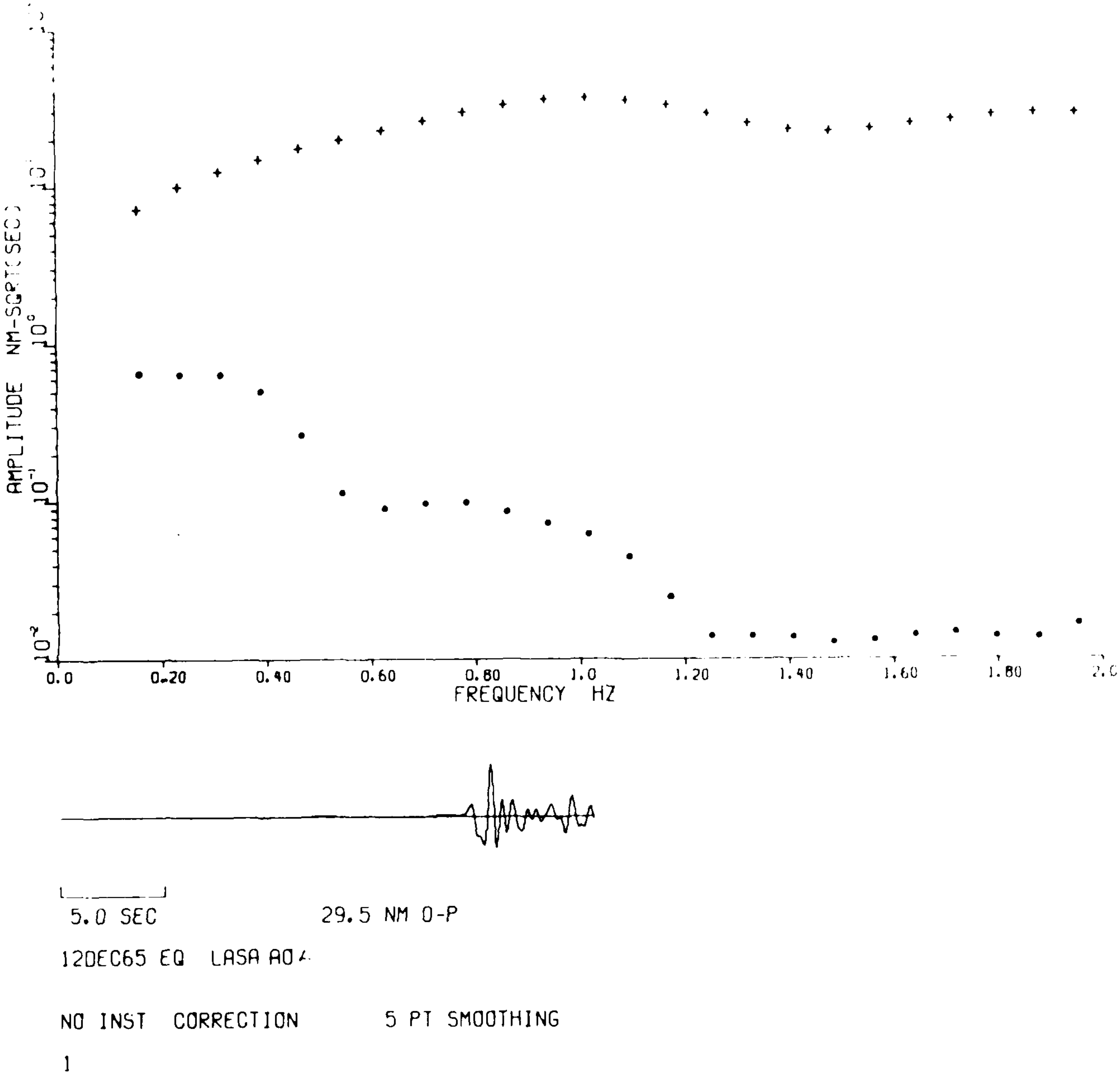

Figure 10. The LASA AO-subarray beamsum spectra for the LONGSHOT P wave and the preceding noise. The plus symbols represent the P-wave spectrum.

AN ANOMALOUS PEAK AT ZERO FREQUENCY IN LASA SHORT-PERIOD SPECTRA

We would like to be able to identify and measure the very low frequency discriminant in the spectra of underground nuclear explosions without having to resort to the spectrum of a control earthquake as a template with which to compare them. That necessity imposes an extra constraint on the use of the discriminant. One objection is that a suitable nearby earthquake may not be available. It is desireable to be able to remove the instrument response and estimated earth response from the shot record to observe and measure the discriminant hole directly. However, in the case of the LASA-LONGSHOT data, upon correcting for the amplitude response of sensor and recorder we find instead of a hole, a spike, or hump, more than 40db above the rest of the spectrum. The significance and the source of the spike are not immediately apparent. It is present not only in the shot spectrum, as, for example, in Figure 11; it is present in the earthquake spectrum, Figure 12; in the spectrum of the beam residual, Figure 13; and in the noise spectrum, Figure 14. In all the spectra the spike is approximately proportional to the rest of the spectrum, i.e., it is present in the spectrum before the arrival of the signal, and when the signal arrives it increases proportionally.

Though it is not at once clear how to account for the observed hump around zero frequency, it is possible to decide whether it is part of the signal. We can do that because our spectra are computed from beamsummed seismograms. An F spectrum is defined for every beamsum, and whether a band of energy in a certain frequency range belongs to the beam may be inferred from that F spectrum. The F spectrum is simply the F statistic as a function of frequency, and the F statistic at a given frequency is the ratio of the energy in the beam to the residual energy at that frequency, all times the number of channels minus 1. For a discussion of the F statistic in signal processing, see Shumway, 1971.

Figure 15 shows an example of one of the LASA-LONGSHOT short-period beamsum spectra and its accompanying F spectrum. Note that the holes due to pP interference

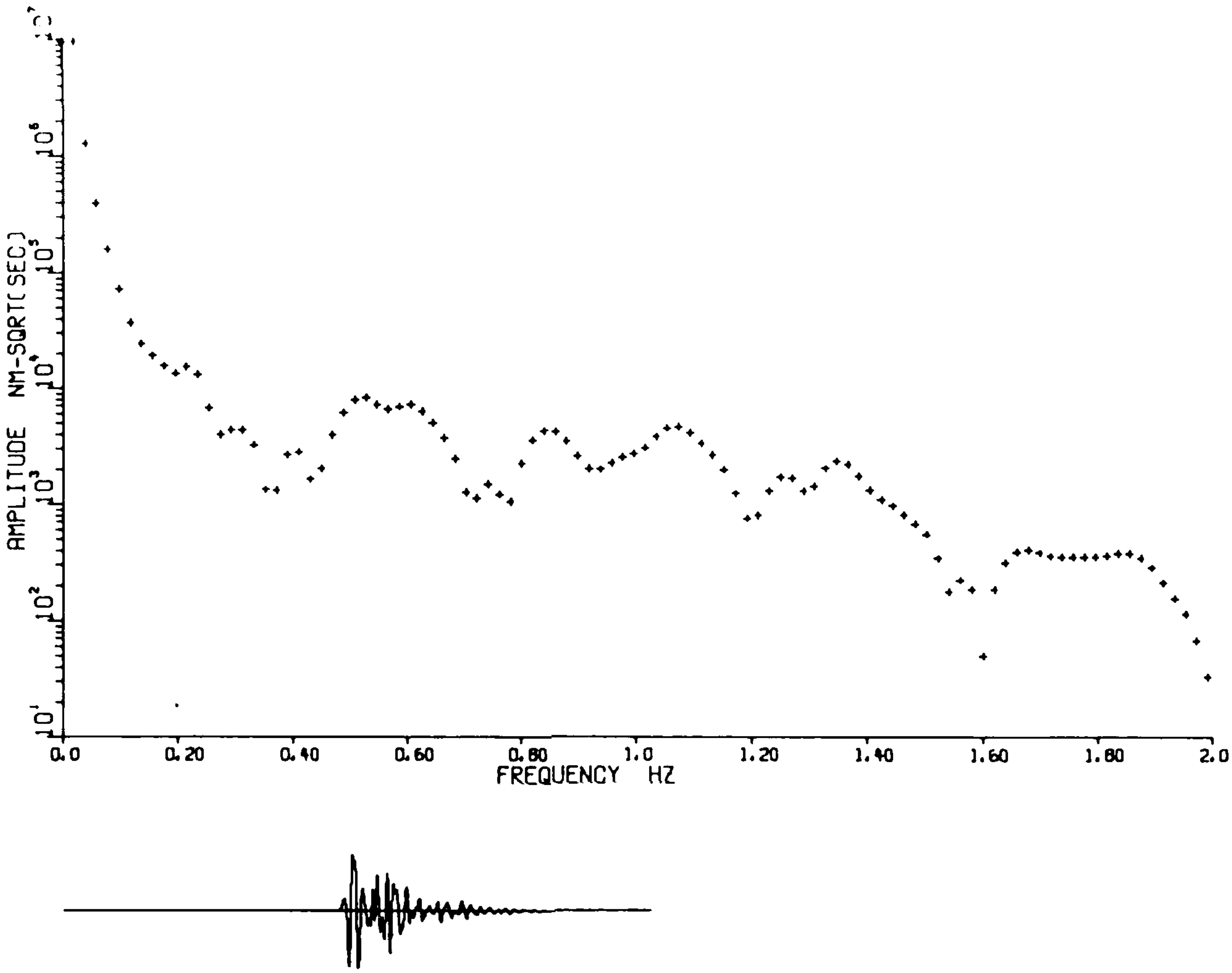

10.0 SEC 172.7 NM O-P

LASA (L23375)

SEISMOGRAM 1 CHANNEL 8

LASA S CORRECTION 0 PT SMOOTHING

2

Figure 11. The LASA D4-subarray beamsum spectrum of LONGSHOT corrected for instrument response. Observe the large peak at zero frequency. Similar anomalous peaks appear in the spectra of the control earthquake, the shot beamsum residuals, and the pre-shot noise, scaled in each case to the rest of the spectrum, as shown in Figures 12, 13, and 14. The window length is 51.2 sec. There is no smoothing.

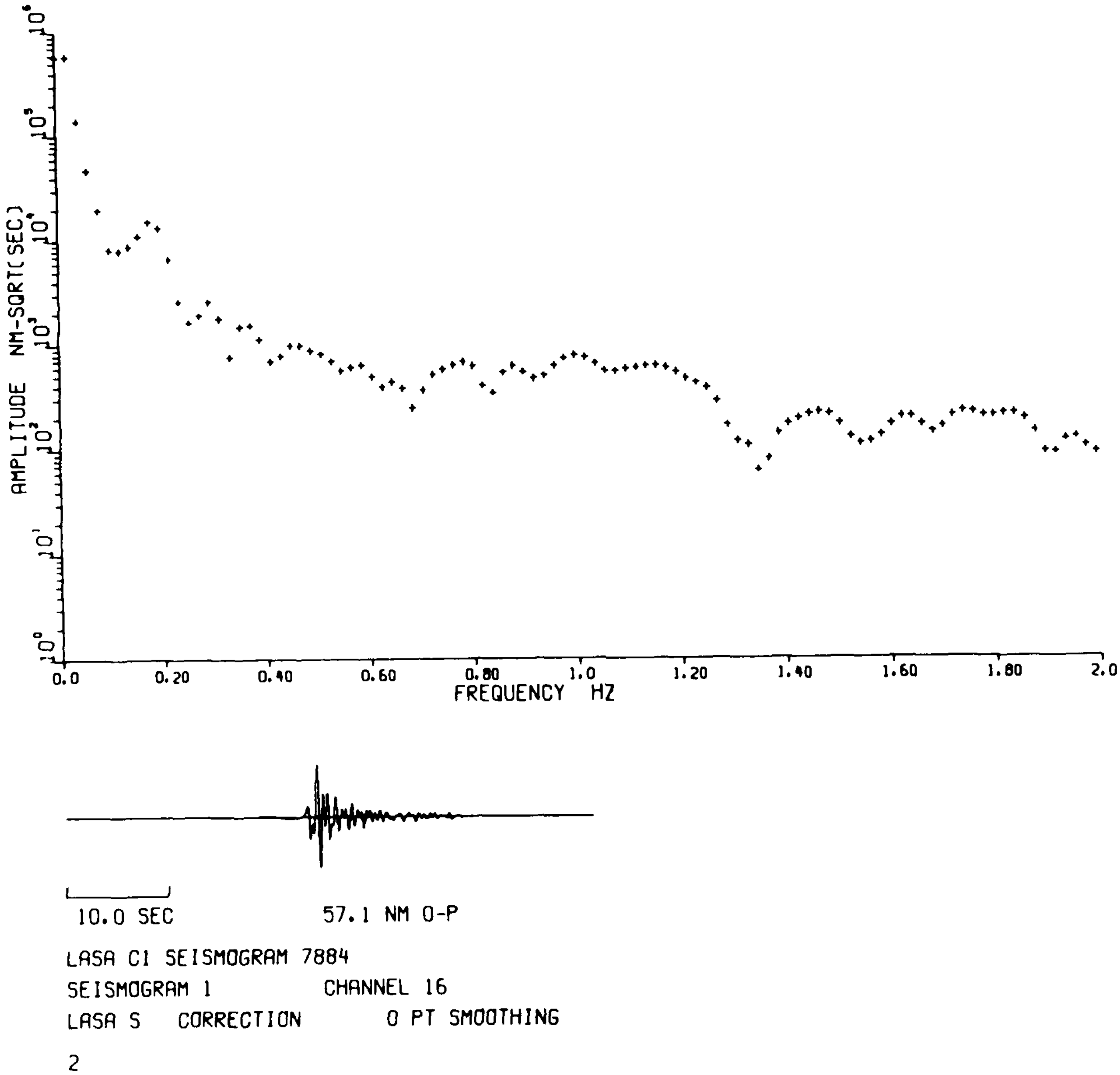

Figure 12. The LASA C1-subarray beamsum spectrum of the control earthquake corrected for instrument response. Observe the peak at zero frequency. Similar anomalous peaks appear in the spectra of LONGSHOT, the shot beamsum residuals, and the pre-shot noise, scaled in each case to the rest of the spectrum, as shown in Figures 11, 13, and 14. The window length is 51.2 sec. There is no smoothing.

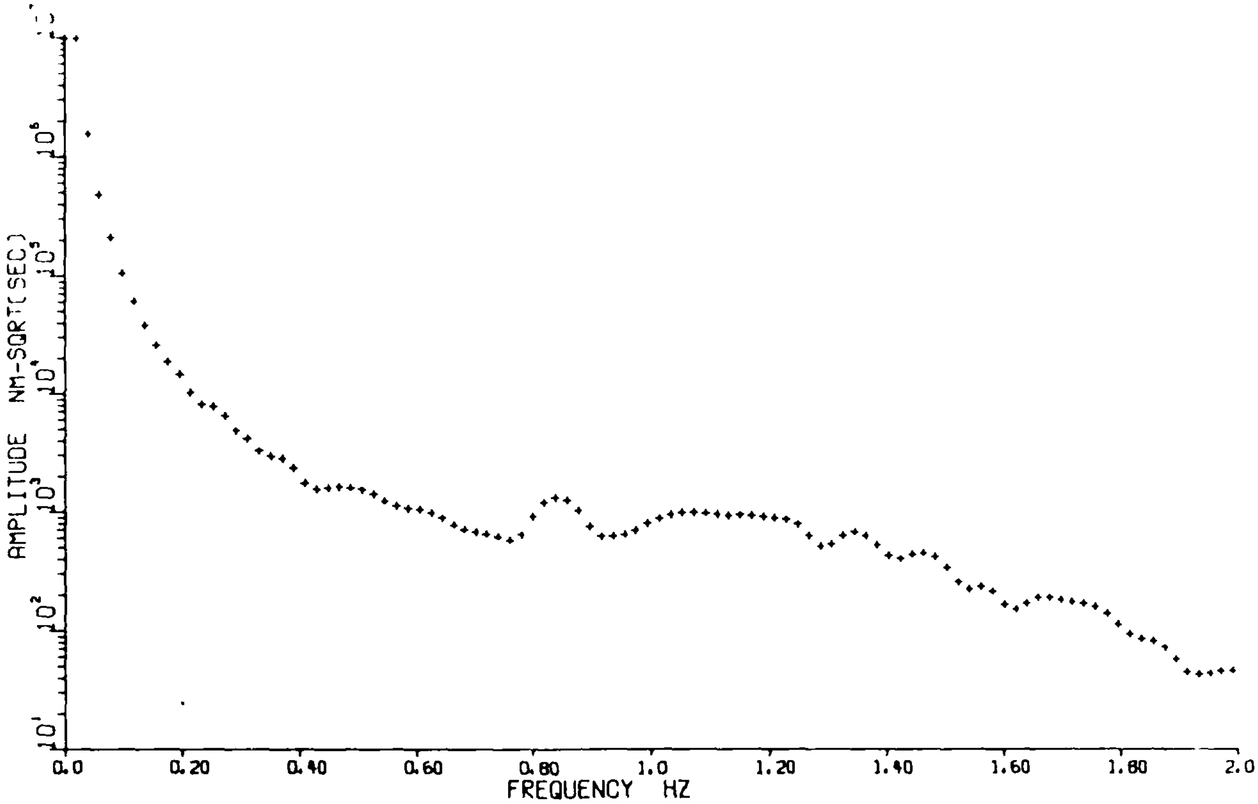

LASA (L23375)

LASA S CORRECTION 0 PT SMOOTHING

1

Figure 13. The mean spectrum of the beamsum residuals of LONGSHOT as recorded at the LASA D4-subarray, corrected for instrument response. Observe the large peak at zero frequency. Similar anomalous peaks appear in the spectra of LONGSHOT itself, the control earthquake, and the pre-shot noise, scaled in each case to the rest of the spectrum, as shown in Figures 11, 12, and 14. The window length is 51.2 sec. There is no smoothing.

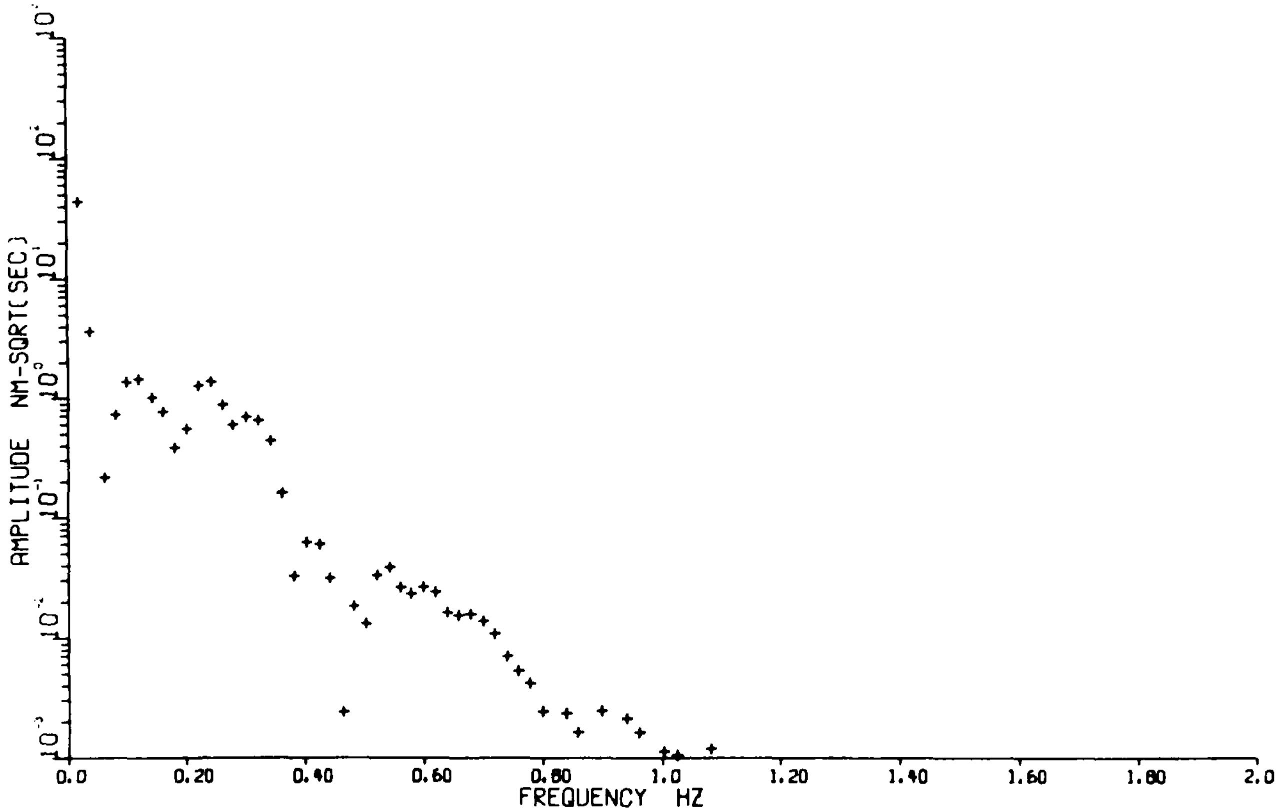

Figure 14. The LASA A0-subarray beamsum spectrum of pre-LONGSHOT noise corrected for instrument response. Observe the peak at zero frequency. Similar anomalous peaks appear in the spectra of LONGSHOT itself, the control earthquake, and the shot beamsum residuals, scaled in each case to the rest of the spectrum, as shown in Figures 11, 12, and 13. The window length is 51.2 sec. There is no smoothing.

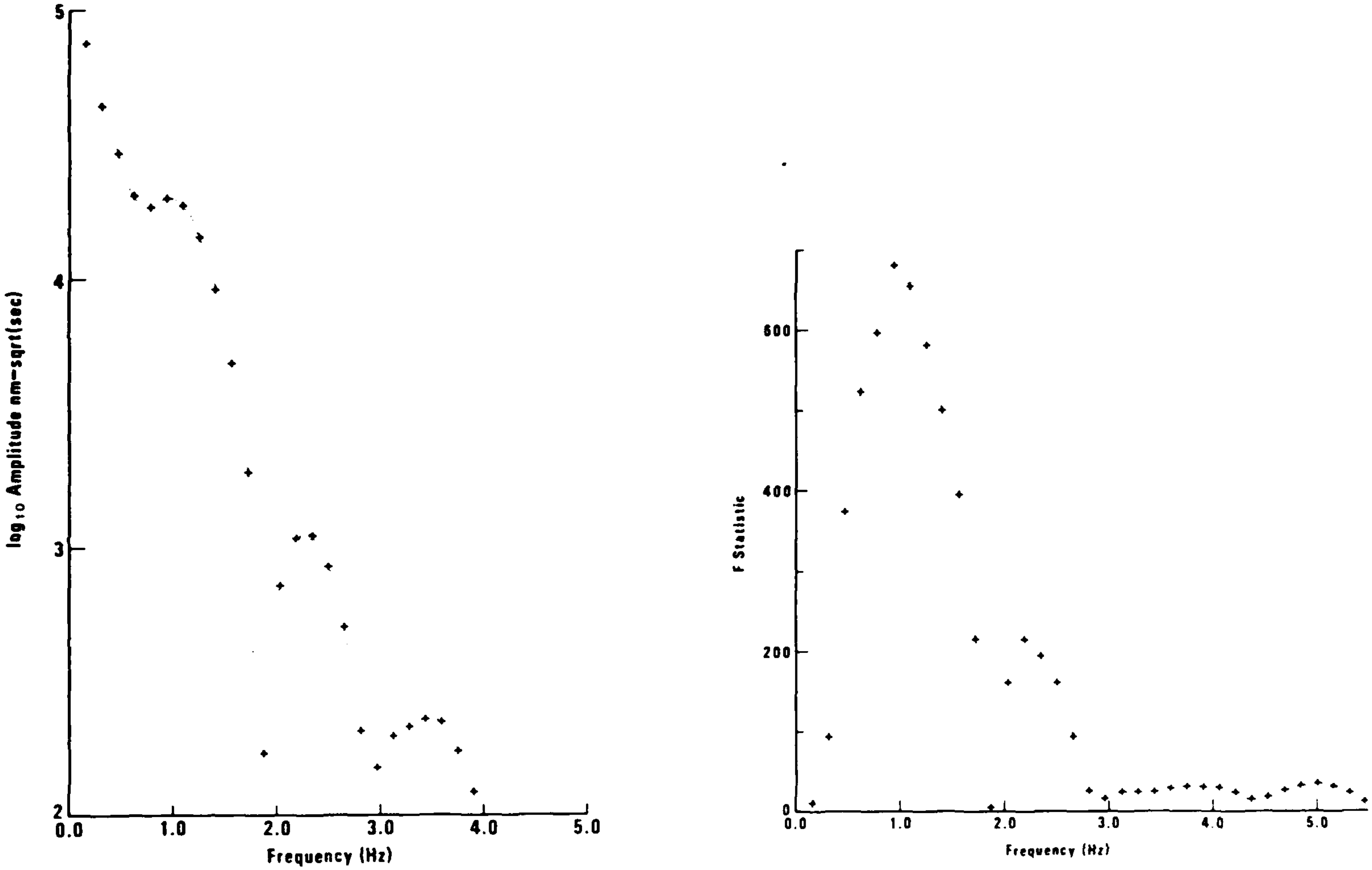

Figure 15. To the left, above, is the LASA AO-subarray beamsum spectrum of the LONGSHOT P-wave corrected for instrument response. Observe the pP hole around 1.9 Hz, and the anomalous peak at zero frequency. The window length is 6.4 sec. There is no smoothing. At the right, above, is the F spectrum for the same window. Observe the pP hole around 1.9 Hz and also that at zero frequency. The latter hole indicates the likelihood that, as zero frequency is approached, less and less of the estimated energy in that part of the spectrum is indeed part of the signal, even though the 25 waveforms in the sum are beamed right at LONGSHOT. This suggests that the F statistic may be used to estimate just how much of the spectral energy at a given frequency is spurious, and to correct for it. That idea is developed in the Appendix.

at very low frequency and at the fundamental frequency are both represented in the F spectrum. The hole at the fundamental frequency, around 1.9 Hz, can be accounted for by the drop to near zero of the amplitude level at that point in the signal spectrum, since the F spectrum is proportional to the estimated signal-to-noise ratio. But there is a hole in the F spectrum at very low frequency as well, in spite of the amplitude maximum at that point. This is accounted for by the residual energy, that is, the energy not in the beam, i.e., noise, which, notwithstanding the magnitude of the energy in the signal spectrum at this point, is so much the greater and reduces the signal-to-noise estimate to near zero.

The significance of the low F statistics in the vicinity of zero frequency is that it is improbable that much of the energy in that band of the estimated signal spectrum is, in reality, part of the signal. So the spectral estimate of the explosion P-wave indicates large amplitude near zero frequency, but its F spectrum shows that that energy probably doesn't belong to the signal after all. Notwithstanding, it has obscured the very low frequency spectral hole we seek.

Thus the large amplitudes near zero frequency, which are orders of magnitude above the rest of the beamsum spectrum, do not belong to signal, that is, they are not organized and are not part of the plane wave, and yet they appear when the signal appears. Nevertheless, the same phenomenon is present in the earthquake records, and so in lieu of explicitly removing this and other extraneous effects, i.e., instrument and earth responses, as we should prefer to do, for the present we can continue to use control earthquake spectra with which to compare the explosion spectra. In effect we are subtracting the log spectrum of the control earthquake from that of the shot, which amounts to dividing out the extraneous effects implicitly. Still, it remains a significant objective to contrive to do all that explicitly, without the control event, since a satisfactory control earthquake may not exist.

CORRECTING FOR BEAMSUM SPECTRAL BIAS

We account for the anomaly of large amplitudes near zero frequency by observing that the beamsum is a biased estimator, notwithstanding its being the optimum estimator for plane waves. Thus beamsumming reduces (but does not eliminate) incoherent noise by a factor of one over the square root of the number of channels, but the noise remnant remains. But that observation suggests that the remnant itself may be estimated and removed from the spectral estimate, correcting the bias, and indeed it can. In the Appendix we develop a function to apply to beamsum spectra which corrects for the bias. The development is based upon, and the bias correction factor is a function of, the F statistic. The factor is (F-1)/F, and, like F, it varies with frequency.

Applied to the spectra of the LONGSHOT P wave, the bias correction indeed removes the very low frequency hump in the LASA beamsum spectra of subarrays B4 and F4, as shown in Figures 16 and 17. (Note that the only other correction applied to these spectra is for the response of the seismometer and recording system.) However, the technique doesn't prove effective for all of the LASA subarray beams. Only 1/3 of them respond. In the case of the others the F statistic around zero frequency is similarly low, but unfortunately not sufficiently low to make the correction factor small enough to effectively suppress the dominant amplitudes in that band. The difficulty remains.

Note that care is taken in the spectral computations to ensure that each window of data has zero mean and zero linear trend, and a window contour is selected to minimize side-lobes. The particular window chosen is one of several optimum windows introduced by Nuttall (1981).

To test the hypothesis that the very low frequency hump is an artifact of the LASA-NORSAR short-period recording system, we recovered the simultaneous recordings of LONGSHOT made on the long-period seismometers at LASA, which were collocated with the short-period subarray center elements. The hypothesis can be at once

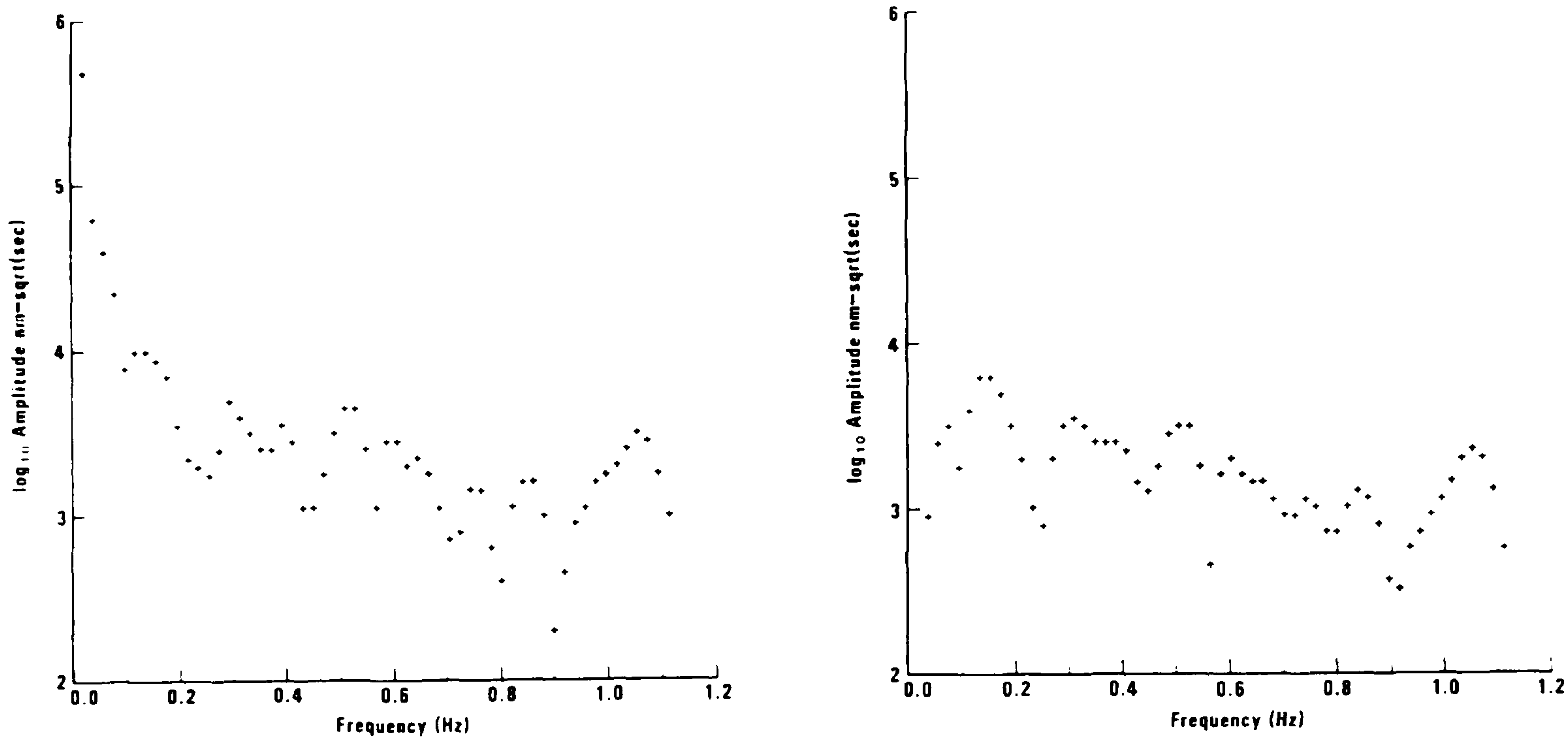

Figure 16. To the left, above, is the LASA B4-subarray beamsum spectrum for LONGSHOT, corrected for instrument response. Observe the sharp peak at zero frequency. The window length is 51.2 sec. There is no smoothing. At the right, above, is the same spectrum corrected for the beamsum bias by means of the F statistic (as a function of frequency). Observe that the sharp peak at zero frequency is now absent, replaced by a hole.

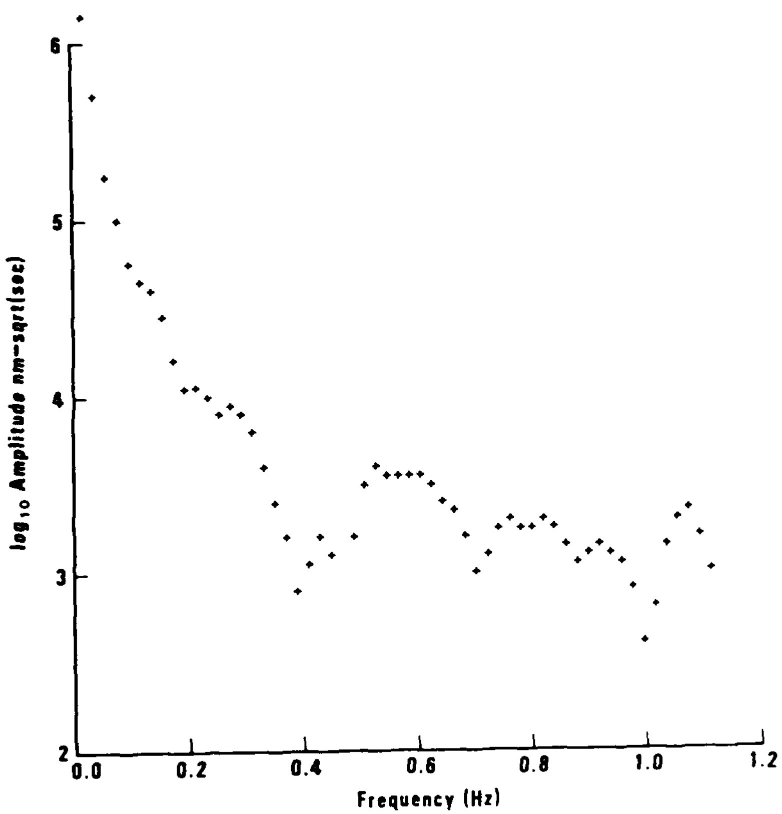

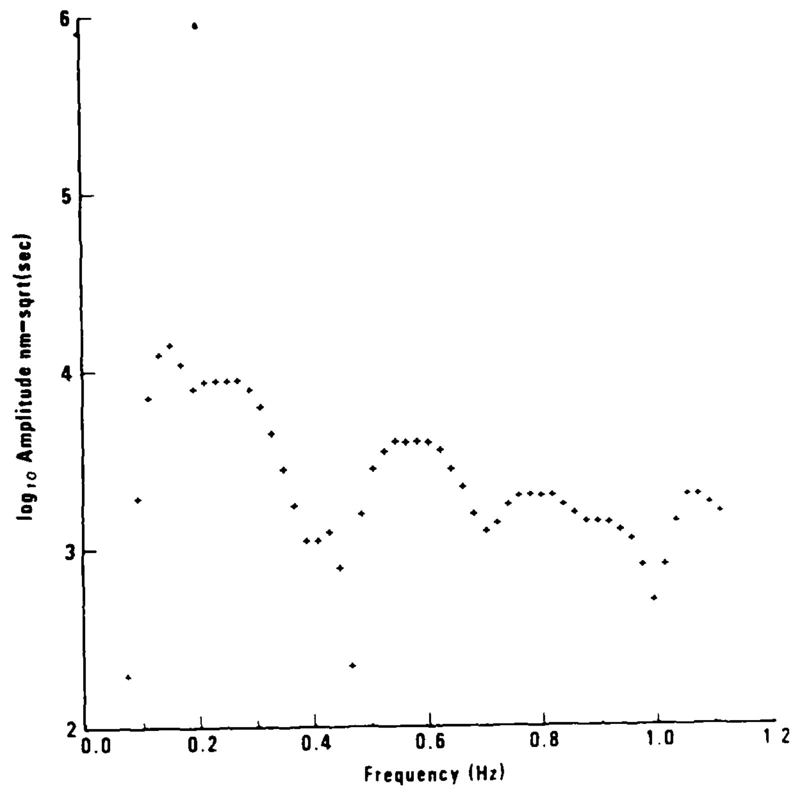

Figure 17. To the left, above, is the LASA F4-subarray beamsum spectrum for LONGSHOT, corrected for instrument response. Observe the large peak at zero frequency. The window length is 51.2 sec. There is no smoothing. At the right, above, is the same spectrum corrected for the beamsum bias by means of the F statistic (as a function of frequency). Observe that the large peak at zero frequency is now absent, replaced by a hole.

substantiated (or definitively eliminated) by comparison of the spectra of simultaneous, identically windowed records of the collocated seismometer pairs. The comparison may also offer a remedy for the problem. Since the response of the short-period system at low frequency is not based on actual field or laboratory measurements but is merely extrapolated from measurements made in the short-period band, and is thus open to question, spectral comparisons offer an alternative calibration technique directly employing the actual response measurements made in that frequency band on the long-period system. Should such calibration of the very low end of the short-period system's response be confirmed by repeated measurements and comparisons with the long-period data, the new measurements would be used to replace the extrapolated calibrations.

CONCLUSIONS AND RECOMMENDATIONS

We have confirmation that the very low frequency discriminant, i.e., the hole at very low frequency due to pP interference in underground nuclear explosion spectra, is preserved in short-period seismic recordings. This is shown repeatedly, from subarray to subarray, in comparisons of LONGSHOT with a control earthquake, in recordings of those events made at LASA. This means that a powerful discriminant, previously neglected, is available with present recording systems. It remains to be seen whether, in application, the discriminant is to be observed directly in the explosion spectra, or will be measured in comparison with spectra of control earthquakes, as in this report.

Microseisms occupy and obscure precisely the spectral band in which we wish to observe the very low frequency discriminant. But both they and the signals of interest are highly organized and well suited to maximum-likelihood array processing which permits the unobstructed observation of one signal in the presence of another. We have developed a linear high-resolution frequency-wavenumber process which operates at the limit of such refinements and is eminently suited to this task, i.e., the resolution of signals not well separated in azimuth and velocity. (Smart, 1976). In its linearity it has an advantage not shared by conventional high-resolution techniques: its spectral estimates are undistorted by non-linear operations. Spectral distortion is a significant and undesirable side effect of non-linear manipulation.

A demonstration of this capacity to recover the low-frequency portion of the spectra of smaller signals in the presence of microseisms, and to reveal the very low frequency discriminant in explosion seismograms is urgently called for.

REFERENCES

Cohen, T. J., (1970). Source-Depth Determinations using Spectral, Pseudo-Autocorrelation and Cepstral Analysis, *Geophys. J. R. astr. Soc. 20*, 223-231.

Douglas, A., D. J. Corbishley, C. Blamey, and P. D. Marshall, (1972). Estimating the Firing Depth of Underground Explosions, *Nature 237*, 26-28.

Nuttall, A. H., (1981). Some Windows with Very Good Sidelobe Behavior, *IEEE ASSP-29*, 84-91.

Shumway, R. H., (1971). On Detecting a Signal in N Stationarily Correlated Noise Series, *Technometrics 13*, 499-519.

Smart, E., (1976). Linear High Resolution Frequency-Wavenumber Analysis, *Doctoral dissertation*, Southern Methodist University.

APPENDIX

The correction for beamsum spectral bias

The expected value of amplitude reduction achieved by summing up N noisy waveforms from an array of seismometers is $\frac{1}{\sqrt{N}}$. (It is assumed that the correlation between waveforms is zero. The amplitudes of the summed waveform are normalized by division by N.)

Thus, notwithstanding that it is an optimum signal estimator, beam summing is biased. It doesn't altogether remove the noise; it reduces it by a factor of $\frac{1}{\sqrt{N}}$ (at best). The remaining noise contaminates resulting spectral estimates of signal. However, that residual noise (which may be larger than the signal in portions of the spectrum) can itself be estimated from the F-statistic. Then an unbiased signal spectrum may be computed.

To calculate a correction factor for the biased spectrum we compute the the expected bias (in the frequency domain) assuming zero correlation between the noise at one station and that at another, and between the signal and the the noise everywhere. The beam-shifted and Fourier transformed array-recording of an event may be represented by d_n, where d is the complex transform coefficient, at a given frequency, of a single channel of data, and n is the channel index of the n^{th} seismometer station.

Let the data be composed of S, the signal itself, plus b_n, the background (noise).

$$d_n = S + b_n \tag{A-1}$$

Since the records are beam-shifted the delay, or step-out, across the array has been removed from the signal, so we take S to be identical from channel to channel. Then the complex Fourier coefficient of the (normalized) beam sum at the given frequency is

$$\frac{1}{N}\sum_{n}^{N} d_n = \frac{1}{N}\sum_{n}^{N} S + b_n \qquad \textbf{(A-2)}$$

(Note that Fourier transforming and summing is identical to summing in the time domain and *then* transforming.) Let the subscripts r and i identify the real and imaginary terms in the complex spectrum. Then the squared magnitude of the coefficient is

$$\left| \frac{1}{N}\sum_{n}^{N} S + b_n \right|^2$$

$$= \frac{1}{N^2}\left(NS_r + \sum_{n}^{N} b_{nr}\right)^2 + \frac{1}{N^2}\left(NS_i + \sum_{n}^{N} b_{ni}\right)^2$$

$$= | S |^2 + \left| \frac{1}{N}\sum_{n}^{N} b_n \right|^2 + \frac{2}{N}\left(S_r \sum_{n}^{N} b_{nr} + S_i \sum_{n}^{N} b_{ni}\right) \qquad \text{(A-3)}$$

Note that the cross terms in $\left| \frac{1}{N}\sum_{n}^{N} b_n \right|^2$ have an expectation of zero by our assumption that the noise correlation between sensors is zero. Then, since the expected value of the third term in (3), above, is also zero, by our assumption of zero correlation between signal and noise, the beam-sum spectral estimate (squared) has the expected value

$$| S |^2 + \frac{1}{N^2}\sum_{n}^{N} | b_n |^2$$

at each frequency.

Similarly, the expectation of

$$\frac{1}{N}\sum_{n}^{N} | d_n |^2 = \frac{1}{N}\sum_{n}^{N} | S + b_n |^2 \qquad \text{(A-4)}$$

is

$$| S |^2 + \frac{1}{N}\sum_{n}^{N} | b_n |^2$$

In the frequency domain the F-statistic for beam sums is defined as

$$F = \frac{(N-1)\left|\frac{1}{N}\sum_{n}^{N} d_n\right|^2}{\frac{1}{N}\sum_{n}^{N} | d_n |^2 - \left|\frac{1}{N}\sum_{n}^{N} d_n\right|^2} \tag{A-5}$$

Substituting our signal model

$$F = \frac{(N-1)\left[| S |^2 + \frac{1}{N^2}\sum_{n}^{N} | b_n |^2\right]}{| S |^2 + \frac{1}{N}\sum_{n}^{N} | b_n |^2 - | S |^2 - \frac{1}{N^2}\sum_{n}^{N} | b_n |^2} \tag{A-6}$$

$$F = \frac{| S |^2 + \frac{1}{N^2}\sum_{n}^{N} | b_n |^2}{\frac{1}{N^2}\sum_{n}^{N} | b_n |^2} \tag{A-7}$$

Thus, with the bias removed, our estimate of the signal amplitude squared, at a given frequency, is

$$| S |^2 = (F-1)\left[\frac{1}{N^2}\sum_{n}^{N} | b_n |^2\right] \tag{A-8}$$

Since

$$F = \frac{| S |^2 + \frac{1}{N^2}\sum_{n}^{N} | b_n |^2}{\frac{1}{N^2}\sum_{n}^{N} | b_n |^2} \tag{A-9}$$

$$\frac{1}{N^2}\sum_{n}^{N} | b_n |^2 = \frac{| S |^2 + \frac{1}{N^2}\sum_{n}^{N} | b_n |^2}{F} = \frac{\left|\frac{1}{N}\sum_{n}^{N} d_n\right|^2}{F} \tag{A-10}$$

and

$$| S |^2 = \frac{(F-1)\left|\frac{1}{N}\sum_{n}^{N} d_n\right|^2}{F} \tag{A-11}$$

$$|S| = \sqrt{(F-1)/F}\left|\frac{1}{N}\sum_{n}^{N} d_n\right| \quad \text{(A-12)}$$

That is, the beam sum amplitude spectrum times the square root of $(F-1)/F$ is an unbiased signal estimate. (Note that $(F-1)/F$ is, of course, frequency dependent.)

Note that the range of expected values of F is from 1 (when $|S|$ goes to zero) to ∞ (when $\sum_{n}^{N} |b_n|^2$ approaches zero). Notwithstanding this range of expected values, ***estimates*** of F can fall below one, in which case the correction factor becomes $(F-1)/F < 0$. Since a negative amplitude spectrum is meaningless, we take the factor to be zero when $F < 1$.

DISTRIBUTION LIST
(UNCLASSIFIED REPORTS)
DARPA FUNDED PROJECTS
(Last Revised 20 Feb 1985)

RECIPIENT	NUMBER OF COPIES
DEPARTMENT OF DEFENSE	
DARPA/GSD 1400 Wilson Boulevard Arlington, VA 22209	2
DARPA/PM 1400 Wilson Boulevard Arlington, VA 22209	1
Defense Technical Information Center Cameron Station Alexandria, VA 22314	12
Defense Intelligence Agency Directorate for Scientific and Technical Intelligence Washington, D.C. 20301	1
Defense Nuclear Agency Shock Physics Directorate/SS Washington, D.C. 20305	1
Defense Nuclear Agency/SPSS ATTN: Dr. Michael Shore 6801 Telegraph Road Alexandria, VA 22310	1
DEPARTMENT OF THE AIR FORCE	
AFGL/LW ATTN: Dr. J. Cipar Terrestrial Sciences Division Hanscom AFB, MA 01730	1
AFOSR/NPG ATTN: Director Bldg 410, Room C222 Bolling AFB, Washington D.C. 20332	1
AFTAC/TG Patrick AFB, FL 32925-6471	4
AFTAC/CA (STINFO) Patrick AFB, FL 32925-6441	1
AFWL/NTESC Kirtland AFB, NM 87171	1

DEPARTMENT OF THE NAVY

NORDA ATTN: Dr. J. A. Ballard Code 543 NSTL Station, MS 39529	1

DEPARTMENT OF ENERGY

Department of Energy ATTN: Dr. F. Dickerson (DP-52) International Security Affairs 1000 Independence Avenue Washington, D.C. 20545	1
Lawrence Livermore National Laboratory ATTN: Dr. J. Hannon and Dr. M. Nordyke University of California P.O. Box 808 Livermore, CA 94550	2
Los Alamos Scientific Laboratory ATTN: Dr. K. Olsen P.O. Box 1663 Los Alamos, NM 87544	1
Sandia Laboratories ATTN: Mr. P. Stokes Geosciences Department 1255 Albuquerque, NM 87115	1

OTHER GOVERNMENT AGENCIES

Central Intelligence Agency ATTN: Dr. L. Turnbull OSI/NED, Room 5G48 Washington, D.C. 20505	1

U.S. Arms Control and Disarmament Agency 2
ATTN: Mrs. M. Hoinkes
Division of Multilateral Affairs
Room 5499
Washington, D.C. 20451

U.S. Geological Survey 1
ATTN: Dr. T. Hanks
National Earthquake Research Center
345 Middlefield Road
Menlo Park, CA 94025

U.S. Geological Survey 1
ATTN: Dr. Robert Masse
Global Seismology Branch
Box 25046, Stop 967
Denver Federal Center
Denver, CO 80225

UNIVERSITIES

University of California, Berkeley 1
ATTN: DR. T. McEvilly
Department of Geology and Geophysics
Berkeley, CA 94720

California Institute of Technology 1
ATTN: Dr. D. Harkrider
Seismological Laboratory
Pasadena, CA 91125

University of California, San Diego 1
ATTN: Dr. J. Orcutt
Scripps Institute of Oceanography
La Jolla, CA 92093

Columbia University 1
ATTN: Dr. L. Sykes
Lamont-Doherty Geological Observatory
Palisades, NY 10964

Massachusetts Institute of Technology 3
ATTN: Dr. S. Soloman, Dr. N. Toksoz, Dr. T. Jordan
Department of Earth and Planetary Sciences
Cambridge, MA 02139

University of Nevada, Reno 1
ATTN: Dr. A. Ryall
Seismological Laboratory
Reno, NV 89557

The Pennsylvania State University 1
ATTN: Dr. S. Alexander
Department of Mineral Sciences
University Park, PN 16802

Southern Methodist University 1
ATTN: Dr. E. Herrin
Geophysical Laboratory
Dallas, TX 75275

CIRES 1
ATTN: Dr. C. Archambeau
University of Colorado
Boulder, CO 80309

Georgia Institute of Technology 1
ATTN: Professor Anton Dainty
The School of Geophysical Sciences
Atlanta, GA 30332

St. Louis University 1
ATTN: Dr. O. Nuttli
Department of Earth and Atmospheric Sciences
3507 Laclede
St. Louis, MO 63156

DEPARTMENT OF DEFENSE CONTRACTORS

Applied Research Associates, Incorporated 1
ATTN: Dr. N. Higgins
2101 San Pedro Boulevard North East
Suite A
Albuquerque, NM 87110

Applied Theory, Incorporated 1
ATTN: Dr. J. Trulio
930 South La Brea Avenue
Suite 2
Los Angeles, CA 90036

Center for Seismic Studies 2
ATTN: Dr. Carl Romney, and Dr. William Dean
1300 N. 17th Street, Suite 1450
Arlington, VA 22209

ENSCO, Incorporated 1
ATTN: Mr. G. Young
5400 Port Royal Road
Springfield, VA 22151

ENSCO, Incorporated 1
ATTN: Dr. R. Kemerait
1930 Highway A1A
Indian Harbour Beach, FL 32937

Pacific Sierra Research Corporation 1
ATTN: Mr. F. Thomas
12340 Santa Monica Boulevard
Los Angeles, CA 90025

R&D Associates 1
ATTN: Dr. E. Martinelli
P.O. Box 9695
Marina del Rey, CA 90291

Rockwell International 1
ATTN: Dr. B. Tittmann
109 Camino Dos Rios
Thousand Oaks, CA 91360

Gould Incorporated 1
ATTN: Mr. R. J. Woodard
Chesapeake Instrument Division
6711 Baymeado Drive
Glen Burnie, MD 21061

Rondout Associates, Incorporated 1
ATTN: Dr. P. Pomeroy
P.O. Box 224
Stone Ridge, NY 12484

Science Applications, Incorporated 1
ATTN: Dr. T. Bache
P.O. Box 2351
La Jolla, CA 92038

Science Horizons
ATTN: Dr. T. Cherry and Dr. J. Minster 2
710 Encinitas Blvd
Suite 101
Encinitas, CA 92024

Sierra Geophysics, Incorporated 2
ATTN: Dr. R. Hart and Dr. G. Mellman
15446 Bell-Red Road
Redmond, WA 98052

SRI International 1
333 Ravensworth Avenue
Menlo Park, CA 94025

S-Cubed, A Division of 1
Maxwell Laboratories Inc.
Attn: Dr. Steven Day
P.O. Box 1620
La Jolla, CA 92038

S-Cubed, A Division of 1
Maxwell Laboratories Inc.
Attn: Mr. J. Murphy
11800 Sunrise Valley Drive
Suite 1212
Reston, VA 22091

Teledyne Geotech
ATTN: Dr. Z. Der & Mr. W. Rivers 2
314 Montgomery Street
Alexandria, VA 22314

Woodward-Clyde Consulants 1
ATTN: Dr. Larry Burdick
556 El Dorado St
Pasadena, CA 91105

Weidlinger Associates 1
ATTN: Dr. J. Isenberg
3000 Sand Hill Road
Menlo Park, CA 94025

NON-U.S. RECIPIENTS

National Defense Research Institute 1
ATTN: Dr. Ola Dahlman
Stockholm 80, Sweden

Blacknest Seismological Center 1
ATTN: Mr. Peter Marshall
Atomic Weapons Research Establishment
UK Ministry of Defense
Brimpton, Reading RG7-4RS
United Kingdom

NTNF NORSAR 1
ATTN: Dr. Frode Ringdal
P.O. Box 51
N-2007 Kjeller
Norway

To be determined by the project office 6